

# NOLO: Navigate Only Look Once

Bohan Zhou  
School of Computer Science  
Peking University  
zhoubh@stu.pku.edu.cn

Jiangxing Wang  
School of Computer Science  
Peking University  
jiangxiw@stu.pku.edu.cn

Zhongbin Zhang  
Department of Automation  
Tsinghua University  
zhangzb23@mails.tsinghua.edu.cn

Zongqing Lu\*  
School of Computer Science  
Peking University  
BAAI  
zongqing.lu@pku.edu.cn

## Abstract

*The in-context learning ability of Transformer models has brought new possibilities to visual navigation. In this paper, we focus on the **video navigation** setting, where an in-context navigation policy needs to be learned purely from videos in an offline manner, without access to the actual environment. For this setting, we propose **Navigate Only Look Once (NOLO)**, a method for learning a navigation policy that possesses the in-context ability and adapts to new scenes by taking corresponding context videos as input without finetuning or re-training. To enable learning from videos, we first propose a pseudo action labeling procedure using optical flow to recover the action label from egocentric videos. Then, offline reinforcement learning is applied to learn the navigation policy. Through extensive experiments on different scenes both in simulation and the real world, we show that our algorithm outperforms baselines by a large margin, which demonstrates the in-context learning ability of the learned policy. For videos and more information, visit our [project page](#).*

## 1. Introduction

Visual navigation has long become a research focus due to its wide application in different fields, including mobile robots [18], autonomous vehicles [38], and virtual assistants [22]. Existing approaches to visual navigation can be broadly divided into two main categories: modular and end-to-end methods. Modular methods decompose the navigation problem into specific tasks, such as simultaneous localization and mapping, object segmentation, keypoint

matching, and depth estimation [14–16, 45, 91]. End-to-end methods [10, 37, 77], on the other hand, bypass such modularization, directly learning the mappings from raw sensory observations (e.g., GPS and Compass [31, 65], RGB-D cameras [34], and IMU [58]) to action outputs. While these approaches have yielded promising results, they still face significant challenges, particularly in terms of generalizability. Modular methods can be brittle when transferred to unfamiliar environments. End-to-end approaches mainly focus on online learning [16, 17, 88], which requires continuous, interactive engagement with simulated or real environments. Thus, they may require additional interactions or exploration to adapt to novel scenes, complicating their deployment in real-world navigation settings.

To address these limitations, it is helpful to consider how humans intuitively navigate. We can often find our way through unfamiliar spaces after watching a simple traversal video. Our navigation abilities do not depend on precise positional data or distance measurement. Instead, we rely primarily on visual recognition, understanding, and memory. Building on this insight, we introduce a new visual navigation setting called **Video Navigation**, which mirrors how humans rely on visual observations to navigate. In video navigation, a mobile agent is provided with a context video of an unfamiliar environment and learns to reach any target seen in the video. For instance, a sweeping robot equipped with video navigation capabilities could immediately navigate and clean any area within a house after viewing a short video of its layout. We believe video navigation has immense potential for endowing mobile agents with human-like navigation capabilities. Although encouraging, achieving robust video navigation poses considerable challenges:

- **Limited Observations.** Learning to navigate from egocentric traversal videos is challenging due to a lack of

\*Corresponding author

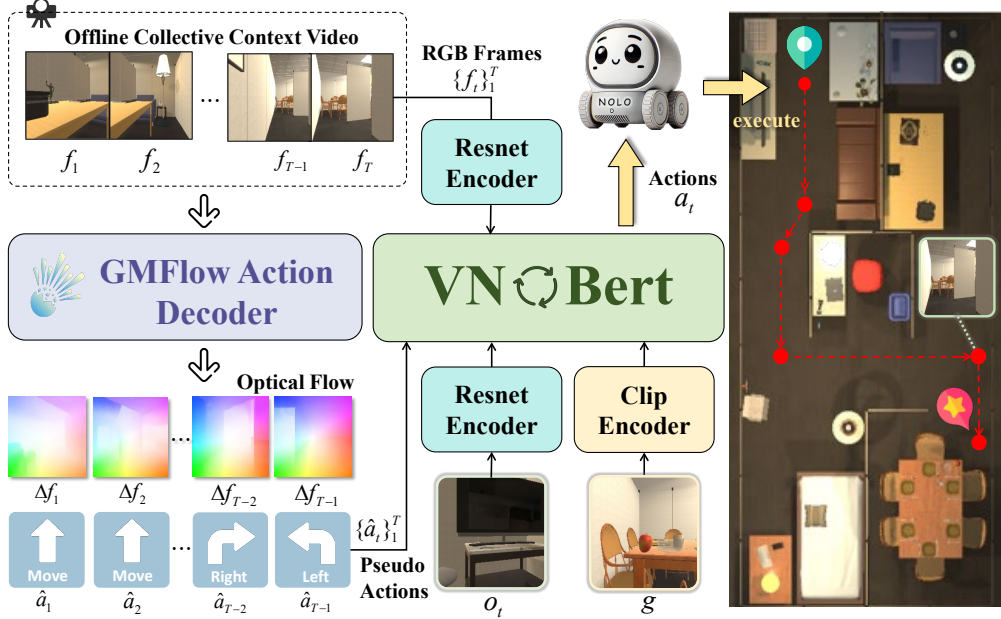


Figure 1. The framework of NOLO. An offline collected egocentric video is taken by a pretrained GMFlow action decoder to label pseudo action sequence  $\{\hat{a}_t\}_1^{T-1}$ . An in-context video navigation policy  $\pi_\theta(\cdot|g, o_t, \{f_t\}_1^T, \{\hat{a}_t\}_1^{T-1})$ , modeled by  $\text{VN}\odot\text{Bert}$ , is learned to take all context frames  $\{f_t\}_1^T$ , labeled actions  $\{\hat{a}_t\}_1^{T-1}$ , a current observation  $o_t$  and a goal image  $g$  to generate discrete actions to navigate to the desired target in a novel scene.

information, including actual actions, spatial cues, scene structure, and visual context.

- **Absence of Explicit Intent.** Egocentric videos lack clear navigational intentions, making conventional methods like inverse reinforcement learning unsuitable, as these approaches typically require expert trajectory data.
- **Minimal Sensory Input.** Camera intrinsics, robot poses, maps, odometers, or depth inputs are not necessary for video navigation, which distinguishes our work from others. A majority of existing methods prefer to build explicit spatial maps for planning with heterogeneous sensors. In this work, we aim to enable human-like navigation using only egocentric RGB observations.

Fundamentally, the objective of video navigation is to train a meta-policy that enables a robot to adapt to a novel scene—essentially, to navigate anywhere using cues from a context video. Recent research demonstrates that in-context learning (ICL [23]) excels at solving tasks using a few contextual demonstrations without requiring additional training [7] and has proven valuable across fields from LLM-based agents [85] to meta-learning [48, 49, 55]. Inspired by the success of ICL, we propose **Navigate Only Look Once (NOLO)**, which learns a transferable in-context navigation policy conditioned on a context video, enabling adaptation to new scenes without fine-tuning or further re-training.

To achieve this, we collect a dataset of egocentric traversal videos, each covering a unique scene. We derive pseudo-actions from these context videos using optical flow, gener-

ating full frame-action trajectories, and then employ an offline reinforcement learning approach to train the navigation policy. This resource-efficient offline training pipeline eliminates the need for time-consuming online interactions, enabling large-scale training on simulated data and facilitating the transfer of navigation skills to unfamiliar environments. Furthermore, NOLO’s in-context adaptability makes it particularly suitable for real-world deployment, where frequent policy adjustments are often impractical.

Our key contributions can be summarized as follows:

- We present a novel and practical setting **Video Navigation**, which necessitates learning an in-context navigation policy in an offline manner purely from videos such that the learned policy can adapt to different scenes by taking corresponding videos as context.
- We propose **NOLO** to solve the video navigation problem. NOLO seamlessly incorporates optical flow into offline reinforcement learning via pseudo-action labeling. To encourage the temporal coherence of representation, we further propose a temporal coherence loss for temporally aligned context visual representation.
- Empirical evaluations on **RoboTHOR** and **Habitat** benchmarks demonstrate the advantages of NOLO over baselines in video navigation. Notably, navigation is achieved by only viewing a single 30-second video clip per scene. We further deploy NOLO on the Unitree Go2 robot and experiments verify that NOLO is also effective and friendly to real-world deployment.

## 2. Related Work

**Visual Navigation.** The visual navigation problem can be categorized into indoor navigation [11, 30, 33, 42, 46, 51, 54, 60, 61, 77, 93] and outdoor navigation [52, 76, 86]. In this paper, we only focus on the indoor navigation problem. Current research mainly focuses on finding the location of specific positions [41, 65], rooms [62], or object instances [41, 44, 45, 50]. The goals of navigation can be described in coordinates [65], natural language [10, 68, 90, 91, 94], goal image of target position [62, 90, 91], or goal image of object instances [41, 43–46, 50, 60]. Our video navigation of finding objects occurred in the context video falls into the last group. Visual navigation methods can also be categorized by whether exploration is required. Most existing works aim for generalization across new goals or environments, heavily relying on learning algorithms that require extensive online interactions, often through reinforcement learning [2, 80, 99], paired with real-time visual feedback [61]. This approach enables the agent to adapt dynamically but requires significant interaction within the environment. Some studies attempt to improve data efficiency but still rely on random policy exploration or assume access to rich datasets, including robot poses [14] or depth images [30, 34, 42, 45]. In contrast, NOLO learns entirely offline. It leverages video data for navigation, freeing the agent from real-world exploration and allowing effective policy learning without performing actual actions, marking a novel approach in video-based visual navigation.

**Learning from Videos.** There are four main lines of research study learning from videos. (1) Learn distinctive representations for intrinsic rewards. These approaches mainly include predicting the future [25, 96, 98], learning temporal abstractions [4, 8, 75, 96], contrastive learning [47, 79], adversarial learning [40, 57, 66, 82] or other transition-learning based methods [6, 53, 64]. (2) Recover value function along with representations [5, 26, 32, 59]. (3) Pretrain action-free model in the first stage and then boost the model with additional action information [74, 87, 92]. (4) Discover latent actions [9, 24, 56, 72] and then align to the real actions online in the environment [24, 56, 72], by human annotation [9] or from offline datasets [72]. Unlike previous work, we focus on the visual navigation problem and by utilizing its specificity, propose an offline method that directly learns the actual navigation policy, not the latent one, from videos. Few attempts are devoted to decoding real actions directly from videos. A recent work AVDC [43] attempts to principally use similar rule-based methods to directly infer actions for robot manipulation. However, it is an online algorithm with additional depth image inputs. We also compare NOLO with AVDC [43] in Sec. 4.5.

**In-Context Learning.** In-context learning (ICL), first demonstrated in large language models [7, 19, 83], enables models to perform new tasks with a few examples as con-

text. This capability has extended to vision-language models [1, 3, 84], AI agents [36, 78], and models across heterogeneous modalities [27, 39]. Our work uniquely applies ICL to video navigation. To our knowledge, NOLO is the first attempt to learn an adaptable policy guided by context videos for diverse scenes.

## 3. Learning to Navigate from Videos

### 3.1. The Problem Formulation of Video Navigation

In video navigation, we offline recover a navigation policy  $\pi_\theta(a|g, o, \mathcal{V})$  to find objects occurred in the context video, which takes a goal image  $g$ , current observation  $o$ , and context video  $\mathcal{V}$  as input and outputs discrete action  $a$ , considering high-level discrete actions are commonly used in competitions like the Habitat Navigation Challenge [69] and modern navigation tasks [52]. To train such a policy, we assume a video dataset  $\mathcal{D}$  contains  $N$  videos collected (e.g., by some simple rule-based policy or humans) in  $N$  different scenes,  $\mathcal{D} = \{\mathcal{V}^1, \mathcal{V}^2, \dots, \mathcal{V}^N\}$ . Each video  $\mathcal{V}^i$  contains  $T$  frames  $f_t^i$ ,  $\mathcal{V}^i = \{f_1^i, f_2^i, \dots, f_T^i\}$ . During inference, we deploy the learned policy in a new scene given a context video  $\mathcal{V}^{\text{new}} \notin \mathcal{D}$  and a goal frame  $g \in \mathcal{G}^{\text{new}}$  describing an object occurred in  $\mathcal{V}^{\text{new}}$ . The policy is expected to adapt to this new scene via in-context learning.

### 3.2. Pseudo Action Labeling

In video navigation, capturing environmental dynamics is crucial for effective adaptation to new scenes. Building on prior work [9, 24, 29, 56, 72] that leverages inverse dynamics models (IDMs) to extract latent actions from adjacent frames, we make a further step by converting latent actions into actual discrete actions within video navigation. Specifically, we propose pseudo action labeling, as illustrated in Fig. 2. we employ GMFlow[89] as an implicit IDM  $F_\xi$  to estimate discrete pixel displacements between consecutive frames and predict real navigation actions from flow maps with rule-based post-processing. For each context video  $\mathcal{V}$ , we label a sequence of pseudo-actions  $\hat{a}$  to get a trajectory  $\mathcal{T} = \{f_t, \hat{a}_t\}_{t=1}^T$ . See Appendix 6.1 for more details.

### 3.3. In-Context Policy Modeling

After labeling pseudo action for all videos, we can build a frame-action dataset to offline train an in-context navigation policy  $\pi_\theta$ . Inspired by VLN-Bert [37], we propose a bidirectional recurrent Transformer, **VN $\odot$ Bert**, to model the in-context navigation policy  $\pi_\theta$ , which can be formalized in Eq. (1):

$$h_{t+1}, \pi_\theta(a_t|g, o_t, \mathcal{T}) = \text{VN} \odot \text{Bert}(g, o_t, \mathcal{T}), \quad (1)$$

where  $h$  is specially designed as a recurrent hidden state to capture informative attention history.

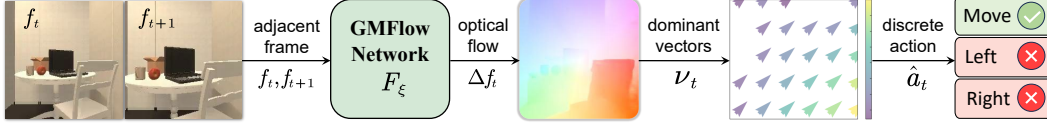


Figure 2. Two adjacent frames are taken by a pretrained optical flow model to get a flow map. Some representative dominant vectors are filtered for action selection.

The structure of  $\text{VN}\odot\text{Bert}$  is depicted in Fig. 3. For inference, all RGB images, including context frames and the current observation are encoded by a learnable ResNet encoder  $E_\zeta$  pretrained from Places365 [95]  $e_t^s = E_\zeta(f_t)$ . Actions are encoded by a learnable action embedding layer  $e_t^a = E_\alpha(\hat{a}_t)$  and the goal frame is encoded by a fixed pretrained CLIP [67]  $e^g = \text{CLIP}(g)$ . During initialization, a zero-padded hidden state  $h_{\text{init}}$  is additionally inserted at the back of the context embedding sequence for recurrence. The entire token embedding sequence  $e_{\text{init}} = [h_{\text{init}}, e_{\text{init},1}^s, e_{\text{init},1}^a, \dots, e_{\text{init},T-1}^s, e_{\text{init},T}^s]$  is encoded by a multi-layer bidirectional self-attention module (SA) as  $e_0 = [e^c, h_0] = \text{SA}(e_{\text{init}})$ . The output feature of the hidden state  $h_0$  serves as the initial compressed representation of the context trajectory. After initialization, the context embedding sequence  $e^c$  keeps unchanged. At each timestep  $t$ , the current observation  $o_t$  and the goal image  $g$  are encoded into  $e_t^s$  and  $e^g$ , respectively. The concatenated embedding sequence  $e_t = [h_t, e^c, e_t^s, e^g]$  is then fed into the cross-attention module (CA) to obtain the updated embedding  $e_{t+1} = \text{CA}(e_t)$  which is further aggregated and projected to action distribution  $\pi_\theta(a_t|g, o_t, \mathcal{T})$  and the next hidden state  $h_{t+1}$ . The updated hidden state  $h_{t+1}$  is subsequently processed by a multilayer perceptron (MLP)  $P_Q$  to regress Q-values  $Q_\omega(g, o_t, a_t, \mathcal{T})$  and by another MLP  $P_D$  to predict the binary terminal signal  $\delta_v(d_t|g, o_t, \mathcal{T})$ , where  $d_t$  is used for predicting the termination of the current task.

To train  $\text{VN}\odot\text{Bert}$ , we sample a context video  $\mathcal{V}^i$  from dataset  $\mathcal{D}$  and then construct a context trajectory  $\mathcal{T}^i = \{f_t^i, \hat{a}_t^i\}_{t=1}^T$  as described in Section 3.2. Then, we randomly sample  $t \in [0, T)$  for a current observation  $o_t$  and pseudo action  $\hat{a}_t$ , and a goal image  $g \in \mathcal{G}^i$ . We set  $d_t = \mathbb{I}(o_t = g)$  for the termination prediction, where  $\mathbb{I}$  is indicator function. We forward the model and calculate discrete action prediction loss and termination prediction loss in Eq. (2),

$$\begin{aligned} \mathcal{L}_a &= -\mathbb{E}_{g, o_t, \hat{a}_t \sim \mathcal{T}^i} \log \pi_\theta(\hat{a}_t | g, o_t, \mathcal{T}^i) \\ \mathcal{L}_d &= -\mathbb{E}_{g, o_t \sim \mathcal{T}^i} \log \delta_v(d_t | g, o_t, \mathcal{T}^i). \end{aligned} \quad (2)$$

### 3.4. Batch-Constrained Q-Learning

Since the policy used to record the video may be highly sub-optimal for video navigation, we favor offline reinforcement learning over imitation learning for policy learning. Specifically, we adopt BCQ [28], an offline reinforcement learning method that emphasizes constraining the action selection to those within the distribution of the observed frame-action

pairs. Q-function  $Q_\omega$  is learned from Bellman update in Eq. (3), where  $r(g, o_t, \hat{a}_t) = \mathbb{I}(o_t = g)$  is a binary reward indicating the success of a task,

$$\begin{aligned} \mathcal{L}_q &= \mathbb{E}_{o_t, o_{t+1}, g, \hat{a}_t \sim \mathcal{T}^i} [Q_\omega(g, o_t, \hat{a}_t, \mathcal{T}^i) - y_t]^2, \\ y_t &= r(g, o_t, \hat{a}_t) + \gamma \max_{\tilde{a}_{t+1} \in A^\beta} Q_\omega(g, o_{t+1}, \tilde{a}_{t+1}, \mathcal{T}^i). \end{aligned} \quad (3)$$

Given the action space is discrete, we define a set  $A^\beta$  in Eq. (4) to select  $\tilde{a}_{t+1}$ , where  $\beta$  represents the threshold for action selection. Action choices are constrained based on the action distribution within the context trajectory dataset. The learned Q-function,  $Q_\omega$ , thus can wisely guides the agent toward the target goal  $g$ .

$$A^\beta := \left\{ \tilde{a}_{t+1} \mid \frac{\pi_\theta(\cdot | g, o_{t+1}, \mathcal{T}^i)}{\max \pi_\theta(\cdot | g, o_{t+1}, \mathcal{T}^i)} > \beta \right\}. \quad (4)$$

### 3.5. Temporal Coherence

Learning temporally aligned representation of videos is crucial for understanding the causality of the context video. Inspired by RLHF [63], we learn a “fuzzy” measure of progress from their natural temporal ordering, where the higher preference score is assigned to the later frames in the video. To achieve this, we learn a temporal indicator  $\hat{u}_\phi(e)$ , which consists of 1D self-attention and spectral normalization modules to map a visual context embedding  $e_t^s$  to a utility score.  $\hat{u}_\phi$  is optimized according to Eq. (5):

$$\min_{\zeta, \phi} \mathcal{L}_t = \mathbb{E}_{f_{t_-}, f_{t_+} \sim \mathcal{V}} -\log \sigma[\hat{u}_\phi(E_\zeta(f_{t_+})) - \hat{u}_\phi(E_\zeta(f_{t_-}))], \quad (5)$$

where  $t_+ > t_-$  and  $f_{t_+}, f_{t_-}$  stands for the later and earlier frame in the video. This self-supervised paradigm naturally drives the temporal indicator  $\hat{u}_\phi(s)$  to maximize likelihood to ensure the temporal order preference  $f_{t_+} \succ f_{t_-}$ , leading to temporally aligned context visual representation, which is beneficial to better understand the temporal relation in a novel scene, as elaborated in later Sec. 4.5.

## 4. Experiments

### 4.1. Experimental Setups

**Configurations.** We apply our algorithm to realistic embodied navigation testbeds RoboTHOR [20] and Habitat [71]. For each navigation task in RoboTHOR and Habitat, we initialize a mobile robot with a random position,

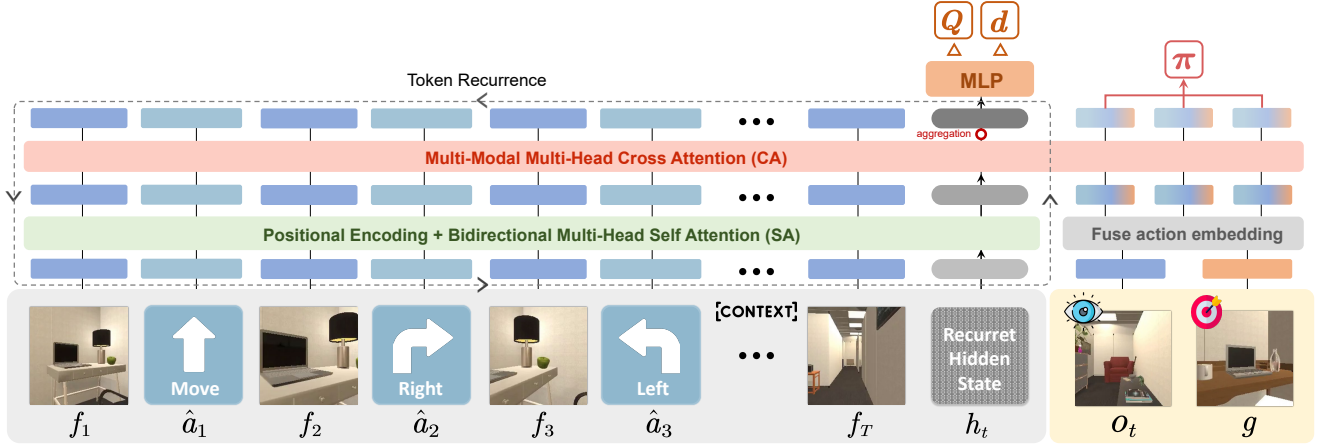


Figure 3. Structure of VN-Bert. At the initialization stage, a trajectory  $\mathcal{T}$  and a zero-padded hidden state  $h_{\text{init}}$  are processed by a bidirectional multi-head self-attention module to obtain context embedding  $e^c$  and initial hidden state  $h_0$ . At each timestep after initialization, the current observation  $o_t$  and goal frame  $g$  are encoded into  $e_t^s$  and are taken by a multi-head cross-attention module together with fixed  $e^c$  and recurrently updated  $h_t$  to produce policy  $\pi_\theta$ , Q-value  $Q_\omega$ , and terminal signal  $\delta_v$ . The red circle indicates additional aggregation via fusing element-wise product between features like VLN-Bert [37].

orientation, and a given goal image extracted from the context video indicating a specific goal object. At each timestep, the agent, mounted with only one RGB camera of  $224 \times 224$  resolution, receives an egocentric image and can execute a discrete action from a fixed action space [MoveForward, TurnLeft, TurnRight, STOP]. The minimum units of rotation and forward movement are  $30^\circ$  and 0.25 meters respectively. When the goal object is observed and the distance between the goal object and the agent is within 1m, the agent succeeds, otherwise it fails when the maximum step is reached, which is 500 in all experiments.

**Task Division.** In RoboTHOR, there are 15 different rooms and 5 possible layouts for each room, in total 75 different scenes. Each room has a different topology from other rooms, and the location of objects in each layout is different from other layouts. In order to test the in-context learning ability at different levels, we divide the training and test scenes as follows. For the training set, we select 12 rooms, and 4 layouts for each room. For the **unseen layout** testing set, we select the remaining 1 layout of the 12 training set rooms, in total 12 scenes. For the **unseen room** testing set, we select the remaining 3 rooms and all their layouts, in total 15 scenes. In Habitat, we divide all 90 building-scale scenes from Matterport3D (MP3D) [12] into 70 training scenes and 20 testing scenes to test the generalization abilities. See Appendix 7.1 for details.

**Dataset Construction.** We use a fixed non-explorative rule-based policy to collect the video dataset. The policy keeps moving forward until colliding with an obstacle and then randomly turns to get rid of it. Simultaneously, the agent keeps recording an egocentric RGB sequence till reaching the maximum 900 steps, *i.e.* a 30-second video clip

in each scene. After that, we employ a pretrained object detector Detic [97] to detect all the objects occurred in the video. To get a set for goal frames, we additionally roll out in the simulation to collect goal images of each target object from different views.

**Task Evaluation.** To evaluate the comprehensive ability of the in-context navigation policy, we design three levels of generalization test:

- Evaluate in the **unseen layout** testing set to test the generalization ability over **layouts**.
- Evaluate in the **unseen room** testing set to test the generalization ability over **rooms**.
- Evaluate in scenes from a different simulator to test the generalization ability over **domains**.

For evaluation, the agent is arranged to navigate to each target object detected in a context video. Each navigation task repeats 10 times.

We conduct 3 runs with different random seeds and quantitatively assess the performance using metrics including success rate (SR), success weighted by normalized inverse path length (SPL), trajectory length (TL), and navigation error (NE) following a recent work [93].

**Baselines.** NOLO stands as the first method to incorporate context videos directly into policy for in-context navigation tasks. To address in-context generalization capabilities, we compare NOLO with a random exploration policy, as well as two large multimodal models (LMMs), GPT-4 and Video-LLaVA which also exhibit remarkable zero-shot multimodal understanding and generation abilities, in a training-free manner. To adapt the LMMs for video-based navigation, we use a queue of size  $K$  to store context video frames, current observations, and goal images, which are

concatenated as LMM input. A unified prompt guides the LMMs to understand the context and navigate effectively in both RoboTHOR and Habitat, extracting actions from their language responses. See Appendix 7.2 for details.

In addition, we further compare NOLO with traditional visual navigation methods without context video input, specifically, an online method VGM [46], which builds a memory graph based on unsupervised image representations from navigation history to guide actions, and an offline method ZSON [60], which encodes goal images into a multimodal, semantic embedding space to enable scalable training of SemanticNav agents in unannotated 3D environments. Besides, we compare NOLO with a recent work AVDC [43], which infers actions from video predictions while incorporating extra depth information. Our experimental results show that AVDC underperforms NOLO even with additional depth images.

## 4.2. RoboTHOR

We average the metrics of video navigation tasks in all testing scenes and showcase the mean results in Tab. 1. NOLO demonstrates overwhelming advantages over baselines, including random, LMM baselines, and visual navigation baselines in both testing sets, which proves its strong generalization abilities to new scenes in different generalization levels. The set of unseen rooms is naturally a harder testing set than the unseen layouts in terms of generalization ability. Therefore, NOLO displays slightly better navigation performance in the unseen layout testing set (71.92% SR, 29.26% SPL) compared to the unseen room testing set (70.48% SR, 27.74% SPL). GPT-4o outperforms the random exploration policy across most scenarios, while VideoLLaVA generally performs below the random exploration policy due to its smaller model size relative to GPT-4o. NOLO is also much more parameter-efficient than GPT-4o. However, it achieves better navigation results, underscoring its effectiveness in training in-context navigation policies. Overall, visual navigation baselines tend to surpass both random and LMM baselines because of additional training. However, AVDC exhibits instability in unseen environments due to its reliance on a diffusion model trained on a limited set of egocentric video frames, which leads to inconsistency in video prediction. While VGM’s memory graph and ZSON’s multimodal semantic embeddings can provide some guidance, they still fall short of NOLO in terms of success rate and path efficiency. We analyzed that VGM’s implicit graph struggles to effectively represent topological structures with limited data coverage, and for ZSON, there is a non-negligible distribution discrepancy between CLIP [67] pre-training data and our egocentric videos. See Figs. 9 and 10 in Appendix 9 for detailed results.

## 4.3. Habitat

We evaluate NOLO similarly in Habitat to demonstrate the effectiveness of NOLO in larger-scale scenes. As illustrated in Tab. 1, NOLO still outperforms baselines in terms of SR and achieves slightly better performance in terms of SPL. Compared with the metrics of NOLO in RoboTHOR, the average SPL and SR are lower, and the average NE and TL are higher. This is mostly because scenes in Habitat are significantly larger than those in RoboTHOR, resulting in more challenging navigation tasks across multiple rooms and even floors and requiring longer traversal distances. However, we observe that NOLO is still capable of acquiring many necessary sub-skills like entering or exiting a room, avoiding obstacles, and exploring. See Appendix 9 for detailed results.

## 4.4. Cross-Domain Evaluation

To pursue the ultimate goal of video navigation, we evaluate NOLO across RoboTHOR and Habitat, even if the visual inputs may suffer from a severe domain gap. Specifically, NOLO trained from 48 RoboTHOR scenes is evaluated in 20 Habitat scenes (**R2H**), and NOLO trained from 70 Habitat scenes is evaluated in 27 RoboTHOR scenes (**H2R**). For comparison, we also plot the average in-domain results (**R2R** and **H2H**). We average all the results on testing scenes in Fig. 4, from which we surprisingly discover that R2H and H2R show competitive performance compared to R2R and H2H. This is because the pretrained image encoder in NOLO provides a general representation of indoor scenes, and the temporal coherence loss in Eq. (5) also leads to a general representation reflecting the natural temporal ordering, which together lead to the generalization ability of NOLO across domains.

## 4.5. Ablation Studies

In this section, we use a set of ablation studies to examine the contribution of several key components in NOLO. More specifically, we aim to answer the following questions.

**Does the context video provide informative cues for navigation? Yes.** We conduct an ablation study denoted as **NOLO-C**, in which we evaluate NOLO without context videos in RoboTHOR and Habitat with other configurations unchanged. From Tab. 2, a mean performance drop of NOLO-C is perceived both in RoboTHOR and Habitat compared with NOLO due to lack of context information.

**Does temporal coherence loss contribute to better visual representation and performance? Yes.** We examine the effect of the temporal coherence loss in Eq. (5). An ablation variant, named **NOLO-T**, is conducted by removing the temporal coherence loss. The results are shown in Tab. 2. The performance drops slightly in RoboTHOR while more obviously in Habitat. To figure out the underlying reasons for their discrepancy in performance, we further compare

Table 1. Performance comparison of success rates (SR), success path lengths (SPL), trajectory lengths (TL), and navigation errors (NE) across different methods and environments. The blue part shows some training-free methods and the green part shows visual navigation approaches which require training.

Method	Robothor								Habitat			
	Unseen Layout				Unseen Room				Unseen Room			
	SR(%) $\uparrow$	SPL(%) $\uparrow$	TL $\downarrow$	NE $\downarrow$	SR(%) $\uparrow$	SPL(%) $\uparrow$	TL $\downarrow$	NE $\downarrow$	SR(%) $\uparrow$	SPL(%) $\uparrow$	TL $\downarrow$	NE $\downarrow$
Random	26.00	13.27	394.77	2.93	23.10	12.02	405.87	2.89	24.53	10.03	402.02	4.97
GPT-4o	31.97	17.18	363.23	3.03	31.69	16.49	364.63	2.89	35.16	20.39	<b>345.84</b>	4.70
Video-LLaVA	20.07	8.31	381.92	3.08	17.51	6.58	385.72	3.32	14.55	9.02	384.53	4.71
AVDC	32.53	9.43	430.77	2.15	31.14	11.57	424.56	2.13	27.29	12.24	418.12	4.30
VGM	47.04	23.90	376.92	2.44	40.51	19.99	400.90	2.38	34.34	17.30	393.92	4.19
ZSON	37.83	21.31	349.31	2.23	35.78	18.81	372.68	2.37	32.83	19.86	395.94	4.32
<b>NOLO (ours)</b>	<b>71.92</b>	<b>29.26</b>	<b>238.92</b>	<b>1.79</b>	<b>70.48</b>	<b>27.74</b>	<b>248.44</b>	<b>1.87</b>	<b>43.65</b>	<b>20.77</b>	347.57	<b>3.67</b>

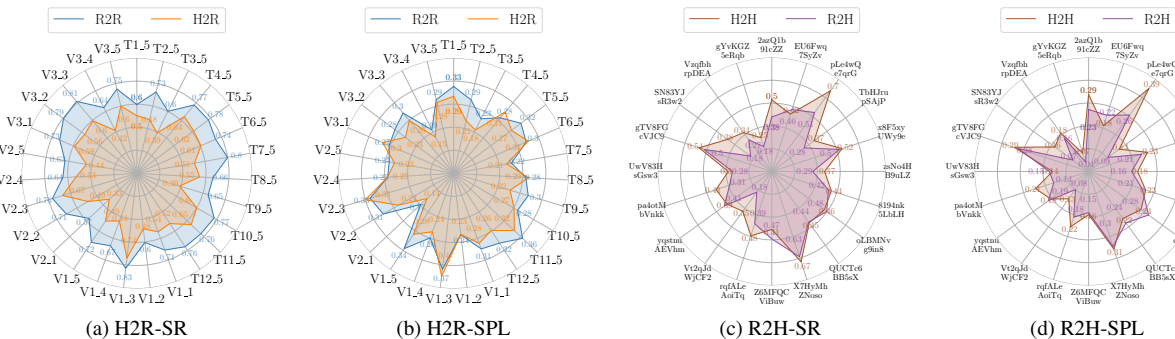


Figure 4. Average SR and SPL of cross domain evaluation. H2R means training in Habitat and testing in RoboTHOR, and vice versa.

the learned visual representation of NOLO and NOLO-T. We randomly select a context video in RoboTHOR and utilize t-SNE projection to visualize their embedding sequences encoded by  $E_{\zeta}(f_t)$  in Fig. 8 in Appendix 8. The embeddings learned by NOLO-T exhibit more irregular stochasticity. In contrast, NOLO learns a better-structured embedding, which demonstrates the effectiveness of the temporal coherence loss. See Appendix 9 for details.

**Can NOLO incorporate other off-the-shelf modules to decode actions from videos? Yes.** We conduct an ablation, entitled NOLO(M), to decode actions from SuperGlue [70] via point matching instead of GMFlow [89]. We observe an accuracy drop in action decoding (from 92.44% to 80.43%). We then follow the same pipeline and report the performance in Tab. 2. NOLO(M) exhibits around 5% decay in average success rate in RoboTHOR and 7% in Habitat. Therefore, to achieve more satisfactory in-context generalization, we choose GMFlow as the action decoder for NOLO. However, as a general two-stage framework for in-context learning from videos, NOLO is not limited to any kind of pseudo action labeling methods and is capable of incorporating more advanced modules for better performance.

**Does NOLO understand the relationship between goal and context video? Yes.** We use Grad-CAM [73] saliency maps of the visual encoder to illustrate NOLO’s ability to

connect the goal with the context video. As shown in Fig. 6, when a goal image is provided, NOLO accurately identifies key semantic cues in the goal and focuses on related areas in the context frame, indicating its capacity to link goal and context. Without the goal image, however, NOLO lacks this focus, underscoring its reliance on goal-driven context understanding. This result demonstrates NOLO’s ability to interpret the goal and capture relevant information in the context video.

#### 4.6. Real-World Experiments

We constructed a real-world maze environment, as shown in Fig. 7. We employed the Unitree Go2 robot, equipped with a RealSense D435i camera to capture RGB observations. In the maze environment, the robot’s actions are discretized into moving forward by 15 cm or turning 30 degrees at each step. Six target objects—a book, box, cola can, cup, glue, and novel—are placed in the maze. Images of each target are taken from random nearby perspectives. A fixed, non-exploratory, rule-based policy was employed to collect two 600-step video clips in the maze, one for training and the other as context video during policy deployment. For evaluation, each episode consists of 100 steps, with a success radius set at 50 cm. Fig. 5 illustrates key frames from successful trajectories during in-context policy deployment.

Table 2. Ablation studies of NOLO. For each method, we average the metrics over all testing scenes and average all the mean results over three random seeds to report the mean and standard deviation.

Method	Robothor				Habitat			
	SR(%) $\uparrow$	SPL(%) $\uparrow$	TL $\downarrow$	NE $\downarrow$	SR(%) $\uparrow$	SPL(%) $\uparrow$	TL $\downarrow$	NE $\downarrow$
NOLO	<b>71.20</b> $\pm$ 0.85	<b>28.50</b> $\pm$ 0.72	<b>243.68</b> $\pm$ 3.80	<b>1.83</b> $\pm$ 0.04	<b>43.65</b> $\pm$ 1.09	<b>20.77</b> $\pm$ 0.46	<b>347.57</b> $\pm$ 3.32	<b>3.67</b> $\pm$ 0.09
NOLO-C	67.78 $\pm$ 0.60	27.70 $\pm$ 1.35	259.65 $\pm$ 0.53	1.98 $\pm$ 0.02	33.58 $\pm$ 0.92	17.41 $\pm$ 0.43	381.26 $\pm$ 3.23	4.58 $\pm$ 0.26
NOLO-T	69.03 $\pm$ 0.87	28.15 $\pm$ 0.09	252.84 $\pm$ 6.33	1.93 $\pm$ 0.04	37.48 $\pm$ 1.01	18.51 $\pm$ 0.71	369.85 $\pm$ 2.72	4.72 $\pm$ 0.07
NOLO(M)	66.15 $\pm$ 0.37	26.66 $\pm$ 1.61	267.95 $\pm$ 1.96	2.02 $\pm$ 0.00	36.73 $\pm$ 1.89	18.17 $\pm$ 0.31	373.92 $\pm$ 3.46	4.69 $\pm$ 0.25

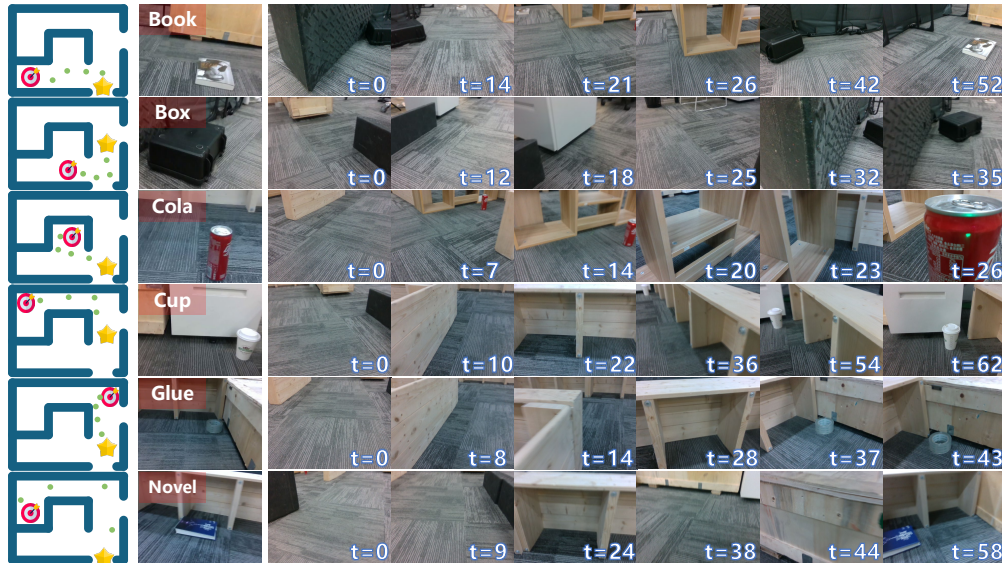


Figure 5. Visualizations of six video navigation tasks during in-context policy deployment. The leftmost bird-eye-view topological maps depicts the robot positions corresponding to the key observations to the right, and the second column displays the goal images.

The robot demonstrated impressive capabilities in navigating straight passages, executing turns at corners, and ultimately reaching the goals by comprehending the dynamics and topological structure inferred from the unseen context video and its relationship to the goal images.

## 5. Conclusion and Limitaiton

In this paper, we propose and investigate the video navigation problem, in which the goal is to offline train a generalizable in-context navigation policy from videos to find objects occurred in a context video about a novel scene. To solve this problem, we propose NOLO, to train a VN $\odot$ Bert taking a context video, current observation, and goal frame as input and outputting navigation actions via pseudo action labeling and offline reinforcement learning. Additionally, we introduce a temporal coherence loss to ensure representations align with natural temporal order. Experiments in RoboTHOR and Habitat simulation environments as well as in a real-world maze demonstrate NOLO can generalize to varying novel scenes without finetuning or re-training by understanding the context video. Ablation studies fur-

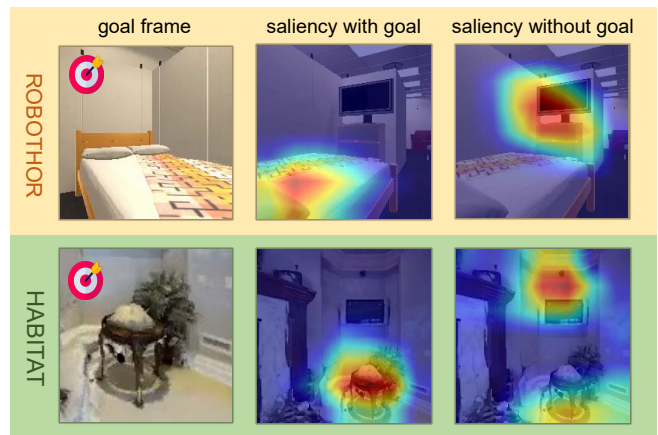


Figure 6. Comparison of saliency maps between NOLO and NOLO-C about context frames with respect to goal frames in RoboTHOR and Habitat.

ther reveal the impact of NOLO’s key components. It is important to emphasize the limitation of NOLO that currently it can only extract movement actions from two adjacent frames. Future work will explore methods for decoding

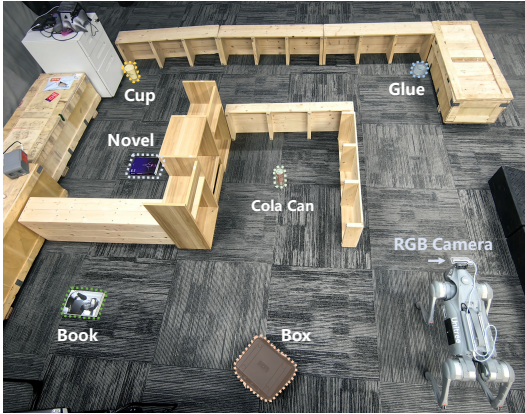


Figure 7. Setups of real-world maze. The robotic dog mounted with a head camera acts as the navigation agent and six annotated objects are goals.

more complex actions from multiple frames. We also aim to pretrain NOLO on larger-scale scene datasets to assess its generalization across more diverse environments.

## References

- [1] Josh Achiam, Steven Adler, Sandhini Agarwal, Lama Ahmad, Ilge Akkaya, Florencia Leoni Aleman, Diogo Almeida, Janko Altenschmidt, Sam Altman, Shyamal Anadkat, et al. Gpt-4 technical report. *arXiv preprint arXiv:2303.08774*, 2023. 3
- [2] Ziad Al-Halah, Santhosh Kumar Ramakrishnan, and Kristen Grauman. Zero experience required: Plug & play modular transfer learning for semantic visual navigation. In *Proceedings of the IEEE/CVF Conference on Computer Vision and Pattern Recognition (CVPR)*, 2022. 3
- [3] Jean-Baptiste Alayrac, Jeff Donahue, Pauline Luc, Antoine Miech, Iain Barr, Yana Hasson, Karel Lenc, Arthur Mensch, Katherine Millican, Malcolm Reynolds, et al. Flamingo: a visual language model for few-shot learning. *Advances in neural information processing systems*, 35:23716–23736, 2022. 3
- [4] Yusuf Aytar, Tobias Pfaff, David Budden, Thomas Paine, Ziyu Wang, and Nando De Freitas. Playing hard exploration games by watching youtube. In *Neural Information Processing Systems (NeurIPS)*, 2018. 3
- [5] Chethan Bhateja, Derek Guo, Dibya Ghosh, Anikait Singh, Manan Tomar, Quan Vuong, Yevgen Chebotar, Sergey Levine, and Aviral Kumar. Robotic offline rl from internet videos via value-function pre-training. *arXiv preprint arXiv:2309.13041*, 2023. 3
- [6] Maksim Bobrin, Nazar Buzun, Dmitrii Krylov, and Dmitry V Dyllov. Align your intents: Offline imitation learning via optimal transport. *arXiv preprint arXiv:2402.13037*, 2024. 3
- [7] Tom Brown, Benjamin Mann, Nick Ryder, Melanie Subbiah, Jared D Kaplan, Prafulla Dhariwal, Arvind Neelakantan, Pranav Shyam, Girish Sastry, Amanda Askell, et al. Language models are few-shot learners. *Advances in neural information processing systems*, 33:1877–1901, 2020. 2, 3
- [8] Jake Bruce, Ankit Anand, Bogdan Mazouze, and Rob Fergus. Learning about progress from experts. In *International Conference on Learning Representations (ICLR)*, 2023. 3
- [9] Jake Bruce, Michael Dennis, Ashley Edwards, Jack Parker-Holder, Yuge Shi, Edward Hughes, Matthew Lai, Aditi Mavalankar, Richie Steigerwald, Chris Apps, et al. Gennie: Generative interactive environments. *arXiv preprint arXiv:2402.15391*, 2024. 3
- [10] Valay Bundele, Mahesh Bhupati, Biplab Banerjee, and Aditya Grover. Scaling vision-and-language navigation with offline rl. *arXiv preprint arXiv:2403.18454*, 2024. 1, 3
- [11] Valay Bundele, Mahesh Bhupati, Biplab Banerjee, and Aditya Grover. Scaling vision-and-language navigation with offline rl. *arXiv preprint arXiv:2403.18454*, 2024. 3
- [12] Angel Chang, Angela Dai, Thomas Funkhouser, Maciej Halber, Matthias Niessner, Manolis Savva, Shuran Song, Andy Zeng, and Yinda Zhang. Matterport3d: Learning from rgb-d data in indoor environments. *International Conference on 3D Vision (3DV)*, 2017. 5
- [13] Matthew Chang, Arjun Gupta, and Saurabh Gupta. Semantic visual navigation by watching youtube videos. In *Neural Information Processing Systems (NeurIPS)*, 2020. 1
- [14] Matthew Chang, Theophile Gervet, Mukul Khanna, Sriram Yenamandra, Dhruv Shah, So Yeon Min, Kavitha Shah, Chris Paxton, Saurabh Gupta, Dhruv Batra, et al. Goat: Go to any thing. *arXiv preprint arXiv:2311.06430*, 2023. 1, 3
- [15] Devendra Singh Chaplot, Dhiraj Gandhi, Saurabh Gupta, Abhinav Gupta, and Ruslan Salakhutdinov. Learning to explore using active neural slam. *arXiv preprint arXiv:2004.05155*, 2020.
- [16] Devendra Singh Chaplot, Ruslan Salakhutdinov, Abhinav Gupta, and Saurabh Gupta. Neural topological slam for visual navigation. In *Proceedings of the IEEE/CVF Conference on Computer Vision and Pattern Recognition (CVPR)*, 2020. 1
- [17] Chang Chen, Yuecheng Liu, Yuzheng Zhuang, Sitong Mao, Kaiwen Xue, and Shunbo Zhou. Scale: Self-correcting visual navigation for mobile robots via anti-novelty estimation. *arXiv preprint arXiv:2404.10675*, 2024. 1
- [18] Chang Chen, Yuecheng Liu, Yuzheng Zhuang, Sitong Mao, Kaiwen Xue, and Shunbo Zhou. Scale: Self-correcting visual navigation for mobile robots via anti-novelty estimation. *arXiv preprint arXiv:2404.10675*, 2024. 1
- [19] Aakanksha Chowdhery, Sharan Narang, Jacob Devlin, Maarten Bosma, Gaurav Mishra, Adam Roberts, Paul Barham, Hyung Won Chung, Charles Sutton, Sebastian Gehrmann, et al. Palm: Scaling language modeling with pathways. *Journal of Machine Learning Research*, 24(240): 1–113, 2023. 3
- [20] Matt Deitke, Winson Han, Alvaro Herrasti, Aniruddha Kembhavi, Eric Kolve, Roozbeh Mottaghi, Jordi Salvador, Dustin Schwenk, Eli VanderBilt, Matthew Wallingford, et al. Rethor: An open simulation-to-real embodied ai platform. In *Proceedings of the IEEE/CVF conference on computer vision and pattern recognition (CVPR)*, pages 3164–3174, 2020. 4
- [21] Jacob Devlin, Ming-Wei Chang, Kenton Lee, and Kristina Toutanova. Bert: Pre-training of deep bidirectional

- transformers for language understanding. *arXiv preprint arXiv:1810.04805*, 2018. 1
- [22] Bernadetta Mustika Dewi, Maya Arlini Puspasari, Billy Muhamad Iqbal, and Tegar Septyan Hidayat. Developing virtual assistant in a virtual retail store environment for product search effectiveness. In *AIP Conference Proceedings*, 2024. 1
- [23] Qingxiu Dong, Lei Li, Damai Dai, Ce Zheng, Zhiyong Wu, Baobao Chang, Xu Sun, Jingjing Xu, and Zhifang Sui. A survey on in-context learning. *arXiv preprint arXiv:2301.00234*, 2022. 2
- [24] Ashley Edwards, Himanshu Sahni, Yannick Schroecker, and Charles Isbell. Imitating latent policies from observation. In *International Conference on Machine Learning (ICML)*, 2019. 3
- [25] Alejandro Escontrela, Ademi Adeniji, Wilson Yan, Ajay Jain, Xue Bin Peng, Ken Goldberg, Youngwoon Lee, Danijar Hafner, and Pieter Abbeel. Video prediction models as rewards for reinforcement learning. *arXiv preprint arXiv:2305.14343*, 2023. 3
- [26] Benjamin Eysenbach, Tianjun Zhang, Sergey Levine, and Russ R Salakhutdinov. Contrastive learning as goal-conditioned reinforcement learning. In *Neural Information Processing Systems (NeurIPS)*, 2022. 3
- [27] Zhongbin Fang, Xiangtai Li, Xia Li, Joachim M Buhmann, Chen Change Loy, and Mengyuan Liu. Explore in-context learning for 3d point cloud understanding. *Advances in Neural Information Processing Systems*, 36, 2024. 3
- [28] Scott Fujimoto, David Meger, and Doina Precup. Off-policy deep reinforcement learning without exploration. In *International Conference on Machine Learning (ICML)*, 2019. 4
- [29] Nathan Gavenski, Juarez Monteiro, Roger Granada, Felipe Meneguzzi, and Rodrigo C Barros. Imitating unknown policies via exploration. *arXiv preprint arXiv:2008.05660*, 2020. 3
- [30] Georgios Georgakis, Yimeng Li, and Jana Kosecka. Simultaneous mapping and target driven navigation. *arXiv preprint arXiv:1911.07980*, 2019. 3
- [31] Theophile Gervet, Soumith Chintala, Dhruv Batra, Jitendra Malik, and Devendra Singh Chaplot. Navigating to objects in the real world. *Science Robotics*, 8(79):eadf6991, 2023. 1
- [32] Dibya Ghosh, Chethan Anand Bhateja, and Sergey Levine. Reinforcement learning from passive data via latent intentions. In *International Conference on Machine Learning (ICML)*. PMLR, 2023. 3
- [33] Pierre-Louis Guhur, Makarand Tapaswi, Shizhe Chen, Ivan Laptev, and Cordelia Schmid. Airbert: In-domain pretraining for vision-and-language navigation. In *Proceedings of the IEEE/CVF conference on Computer Vision and Pattern Recognition (CVPR)*, 2021. 3
- [34] Meera Hahn, Devendra Singh Chaplot, Shubham Tulsiani, Mustafa Mukadam, James M Rehg, and Abhinav Gupta. No rl, no simulation: Learning to navigate without navigating. In *Neural Information Processing Systems (NeurIPS)*, 2021. 1, 3
- [35] Weituo Hao, Chunyuan Li, Xiujun Li, Lawrence Carin, and Jianfeng Gao. Towards learning a generic agent for vision-and-language navigation via pre-training. In *Proceedings of the IEEE/CVF conference on Computer Vision and Pattern Recognition (CVPR)*, 2020. 1
- [36] Sirui Hong, Xiawu Zheng, Jonathan Chen, Yuheng Cheng, Jinlin Wang, Ceyao Zhang, Zili Wang, Steven Ka Shing Yau, Zijuan Lin, Liyang Zhou, et al. Metagpt: Meta programming for multi-agent collaborative framework. *arXiv preprint arXiv:2308.00352*, 2023. 3
- [37] Yicong Hong, Qi Wu, Yuankai Qi, Cristian Rodriguez-Opazo, and Stephen Gould. Vln bert: A recurrent vision-and-language bert for navigation. In *Proceedings of the IEEE/CVF conference on Computer Vision and Pattern Recognition (CVPR)*, pages 1643–1653, 2021. 1, 3, 5
- [38] Dong Hu, Chao Huang, Jingda Wu, and Hongbo Gao. Pre-trained transformer-enabled strategies with human-guided fine-tuning for end-to-end navigation of autonomous vehicles. *arXiv preprint arXiv:2402.12666*, 2024. 1
- [39] Qian Huang, Hongyu Ren, Peng Chen, Gregor Kržmanc, Daniel Zeng, Percy S Liang, and Jure Leskovec. Prodigy: Enabling in-context learning over graphs. *Advances in Neural Information Processing Systems*, 36, 2024. 3
- [40] Haresh Karnan, Garrett Warnell, Faraz Torabi, and Peter Stone. Adversarial imitation learning from video using a state observer. In *International Conference on Robotics and Automation (ICRA)*, 2022. 3
- [41] Apoorv Khandelwal, Luca Weihs, Roozbeh Mottaghi, and Aniruddha Kembhavi. Simple but effective: Clip embeddings for embodied ai. In *Proceedings of the IEEE/CVF Conference on Computer Vision and Pattern Recognition (CVPR)*, pages 14829–14838, 2022. 3
- [42] Nuri Kim, Obin Kwon, Hwiyeon Yoo, Yunho Choi, Jeongho Park, and Songhwai Oh. Topological semantic graph memory for image-goal navigation. In *Conference on Robot Learning*, pages 393–402. PMLR, 2023. 3
- [43] Po-Chen Ko, Jiayuan Mao, Yilun Du, Shao-Hua Sun, and Joshua B Tenenbaum. Learning to act from actionless videos through dense correspondences. *arXiv preprint arXiv:2310.08576*, 2023. 3, 6
- [44] Jacob Krantz, Stefan Lee, Jitendra Malik, Dhruv Batra, and Devendra Singh Chaplot. Instance-specific image goal navigation: Training embodied agents to find object instances. *arXiv preprint arXiv:2211.15876*, 2022. 3
- [45] Jacob Krantz, Theophile Gervet, Karmesh Yadav, Austin Wang, Chris Paxton, Roozbeh Mottaghi, Dhruv Batra, Jitendra Malik, Stefan Lee, and Devendra Singh Chaplot. Navigating to objects specified by images. In *Proceedings of the IEEE/CVF International Conference on Computer Vision (CVPR)*, 2023. 1, 3
- [46] Obin Kwon, Nuri Kim, Yunho Choi, Hwiyeon Yoo, Jeongho Park, and Songhwai Oh. Visual graph memory with unsupervised representation for visual navigation. In *Proceedings of the IEEE/CVF international conference on computer vision*, pages 15890–15899, 2021. 3, 6
- [47] Michael Laskin, Aravind Srinivas, and Pieter Abbeel. Curl: Contrastive unsupervised representations for reinforcement learning. In *International Conference on Machine Learning (ICML)*, 2020. 3
- [48] Michael Laskin, Luyu Wang, Junhyuk Oh, Emilio Parisotto, Stephen Spencer, Richie Steigerwald, DJ Strouse, Steven

- Hansen, Angelos Filos, Ethan Brooks, et al. In-context reinforcement learning with algorithm distillation. *arXiv preprint arXiv:2210.14215*, 2022. 2
- [49] Jonathan Lee, Annie Xie, Aldo Pacchiano, Yash Chandak, Chelsea Finn, Ofir Nachum, and Emma Brunskill. Supervised pretraining can learn in-context reinforcement learning. In *Neural Information Processing Systems (NeurIPS)*, 2024. 2
- [50] Xiaohan Lei, Min Wang, Wengang Zhou, Li Li, and Houqiang Li. Instance-aware exploration-verification-exploitation for instance imagegoal navigation. *arXiv preprint arXiv:2402.17587*, 2024. 3
- [51] Hongxin Li, Zeyu Wang, Xu Yang, Yuran Yang, Shuqi Mei, and Zhaoxiang Zhang. Memonav: Working memory model for visual navigation. In *Proceedings of the IEEE/CVF Conference on Computer Vision and Pattern Recognition*, pages 17913–17922, 2024. 3
- [52] Jialu Li, Aishwarya Padmakumar, Gaurav Sukhatme, and Mohit Bansal. Vln-video: Utilizing driving videos for outdoor vision-and-language navigation. *arXiv preprint arXiv:2402.03561*, 2024. 3
- [53] Siyuan Li, Shijie Han, Yingnan Zhao, By Liang, and Peng Liu. Auxiliary reward generation with transition distance representation learning. *arXiv preprint arXiv:2402.07412*, 2024. 3
- [54] Yimeng Li and Jana Kořecka. Learning view and target invariant visual servoing for navigation. In *2020 IEEE International Conference on Robotics and Automation (ICRA)*, pages 658–664. IEEE, 2020. 3
- [55] Hao Liu and Pieter Abbeel. Emergent agentic transformer from chain of hindsight experience. In *International Conference on Machine Learning*, 2023. 2
- [56] Minghuan Liu, Zhengbang Zhu, Yuzheng Zhuang, Weinan Zhang, Jianye Hao, Yong Yu, and Jun Wang. Plan your target and learn your skills: Transferable state-only imitation learning via decoupled policy optimization. *arXiv preprint arXiv:2203.02214*, 2022. 3
- [57] Minghuan Liu, Tairan He, Weinan Zhang, Shuicheng Yan, and Zhongwen Xu. Visual imitation learning with patch rewards. *arXiv preprint arXiv:2302.00965*, 2023. 3
- [58] Pin Lyu, Bingqing Wang, Jizhou Lai, Shiyu Bai, Ming Liu, and Wenbin Yu. A factor graph optimization method for high-precision imu based navigation system. *IEEE Transactions on Instrumentation and Measurement*, 2023. 1
- [59] Yecheng Jason Ma, Shagun Sodhani, Dinesh Jayaraman, Osbert Bastani, Vikash Kumar, and Amy Zhang. Vip: Towards universal visual reward and representation via value-implicit pre-training. *arXiv preprint arXiv:2210.00030*, 2022. 3
- [60] Arjun Majumdar, Gunjan Aggarwal, Bhavika Devnani, Judy Hoffman, and Dhruv Batra. Zson: Zero-shot object-goal navigation using multimodal goal embeddings. *Advances in Neural Information Processing Systems*, 35:32340–32352, 2022. 3, 6
- [61] Bar Mayo, Tamir Hazan, and Ayellet Tal. Visual navigation with spatial attention. In *Proceedings of the IEEE/CVF conference on computer vision and pattern recognition*, pages 16898–16907, 2021. 3
- [62] Lina Mezghan, Sainbayar Sukhbaatar, Thibaut Lavril, Oleksandr Maksymets, Dhruv Batra, Piotr Bojanowski, and Kar-teek Alahari. Memory-augmented reinforcement learning for image-goal navigation. In *IEEE/RSJ International Conference on Intelligent Robots and Systems (IROS)*, 2022. 3
- [63] Long Ouyang, Jeffrey Wu, Xu Jiang, Diogo Almeida, Carroll Wainwright, Pamela Mishkin, Chong Zhang, Sandhini Agarwal, Katarina Slama, Alex Ray, et al. Training language models to follow instructions with human feedback. In *Neural Information Processing Systems (NeurIPS)*, 2022. 4
- [64] Seohong Park, Tobias Kreiman, and Sergey Levine. Foundation policies with hilbert representations. *arXiv preprint arXiv:2402.15567*, 2024. 3
- [65] Ruslan Partsey, Erik Wijmans, Naoki Yokoyama, Oles Dobosevych, Dhruv Batra, and Oleksandr Maksymets. Is mapping necessary for realistic pointgoal navigation? In *Proceedings of the IEEE/CVF Conference on Computer Vision and Pattern Recognition (CVPR)*, 2022. 1, 3
- [66] Xue Bin Peng, Ze Ma, Pieter Abbeel, Sergey Levine, and Angjoo Kanazawa. Amp: Adversarial motion priors for stylized physics-based character control. *ACM Transactions on Graphics (ToG)*, 40(4):1–20, 2021. 3
- [67] Alec Radford, Jong Wook Kim, Chris Hallacy, Aditya Ramesh, Gabriel Goh, Sandhini Agarwal, Girish Sastry, Amanda Askell, Pamela Mishkin, Jack Clark, et al. Learning transferable visual models from natural language supervision. In *International Conference on Machine Learning (ICML)*, 2021. 4, 6
- [68] Santhosh Kumar Ramakrishnan, Devendra Singh Chaplot, Ziad Al-Halah, Jitendra Malik, and Kristen Grauman. Poni: Potential functions for objectgoal navigation with interaction-free learning. In *Proceedings of the IEEE/CVF Conference on Computer Vision and Pattern Recognition (CVPR)*, 2022. 3
- [69] Ram Ramrakhya, Eric Undersander, Dhruv Batra, and Abhishek Das. Habitat-web: Learning embodied object-search strategies from human demonstrations at scale. In *Proceedings of the IEEE/CVF conference on Computer Vision and Pattern Recognition (CVPR)*, 2022. 3
- [70] Paul-Edouard Sarlin, Daniel DeTone, Tomasz Malisiewicz, and Andrew Rabinovich. Superglue: Learning feature matching with graph neural networks. In *Proceedings of the IEEE/CVF conference on computer vision and pattern recognition (CVPR)*, 2020. 7
- [71] Manolis Savva, Abhishek Kadian, Oleksandr Maksymets, Yili Zhao, Erik Wijmans, Bhavana Jain, Julian Straub, Jia Liu, Vladlen Koltun, Jitendra Malik, et al. Habitat: A platform for embodied ai research. In *Proceedings of the IEEE/CVF International Conference on Computer Vision (CVPR)*, 2019. 4
- [72] Dominik Schmidt and Minqi Jiang. Learning to act without actions. *arXiv preprint arXiv:2312.10812*, 2023. 3
- [73] Ramprasaath R Selvaraju, Michael Cogswell, Abhishek Das, Ramakrishna Vedantam, Devi Parikh, and Dhruv Batra. Grad-cam: Visual explanations from deep networks via gradient-based localization. In *International Conference on Computer Vision (ICCV)*, 2017. 7

- [74] Younggyo Seo, Kimin Lee, Stephen L James, and Pieter Abbeel. Reinforcement learning with action-free pre-training from videos. In *International Conference on Machine Learning (ICML)*, 2022. 3
- [75] Pierre Sermanet, Corey Lynch, Yevgen Chebotar, Jasmine Hsu, Eric Jang, Stefan Schaal, Sergey Levine, and Google Brain. Time-contrastive networks: Self-supervised learning from video. In *IEEE International Conference on Robotics and Automation (ICRA)*, 2018. 3
- [76] Dhruv Shah, Błażej Osiniński, Sergey Levine, et al. Lmnav: Robotic navigation with large pre-trained models of language, vision, and action. In *Conference on Robot Learning (CORL)*, 2023. 3
- [77] Dhruv Shah, Ajay Sridhar, Nitish Dashora, Kyle Stachowicz, Kevin Black, Noriaki Hirose, and Sergey Levine. Vint: A foundation model for visual navigation. In *Conference on Robot Learning*, pages 711–733. PMLR, 2023. 1, 3
- [78] Yongliang Shen, Kaitao Song, Xu Tan, Dongsheng Li, Weiming Lu, and Yueting Zhuang. Hugginggpt: Solving ai tasks with chatgpt and its friends in hugging face. *Advances in Neural Information Processing Systems*, 36, 2024. 3
- [79] Adam Stooke, Kimin Lee, Pieter Abbeel, and Michael Laskin. Decoupling representation learning from reinforcement learning. In *International Conference on Machine Learning (ICML)*, 2021. 3
- [80] Xinyu Sun, Peihao Chen, Jugang Fan, Jian Chen, Thomas Li, and Mingkui Tan. Fgprompt: Fine-grained goal prompting for image-goal navigation. In *Neural Information Processing Systems (NeurIPS)*, 2024. 3
- [81] Hao Tan and Mohit Bansal. Lxmert: Learning cross-modality encoder representations from transformers. *arXiv preprint arXiv:1908.07490*, 2019. 1
- [82] Faraz Torabi, Garrett Warnell, and Peter Stone. Imitation learning from video by leveraging proprioception. In *International Joint Conference on Artificial Intelligence (IJCAI)*, 2019. 3
- [83] Hugo Touvron, Thibaut Lavril, Gautier Izacard, Xavier Martinet, Marie-Anne Lachaux, Timothée Lacroix, Baptiste Rozière, Naman Goyal, Eric Hambro, Faisal Azhar, et al. Llama: Open and efficient foundation language models. *arXiv preprint arXiv:2302.13971*, 2023. 3
- [84] Maria Tsimpoukelli, Jacob L Menick, Serkan Cabi, SM Eslami, Oriol Vinyals, and Felix Hill. Multimodal few-shot learning with frozen language models. *Advances in Neural Information Processing Systems*, 34:200–212, 2021. 3
- [85] Lei Wang, Chen Ma, Xueyang Feng, Zeyu Zhang, Hao Yang, Jingsen Zhang, Zhiyuan Chen, Jiakai Tang, Xu Chen, Yankai Lin, et al. A survey on large language model based autonomous agents. *Frontiers of Computer Science*, 18(6):1–26, 2024. 2
- [86] Justin Wasserman, Karmesh Yadav, Girish Chowdhary, Abhinav Gupta, and Unnat Jain. Last-mile embodied visual navigation. In *Conference on Robot Learning*, pages 666–678. PMLR, 2023. 3
- [87] Jialong Wu, Haoyu Ma, Chaoyi Deng, and Mingsheng Long. Pre-training contextualized world models with in-the-wild videos for reinforcement learning. In *Neural Information Processing Systems (NeurIPS)*, 2024. 3
- [88] Chengguang Xu, Hieu T Nguyen, Christopher Amato, and Lawson LS Wong. Vision and language navigation in the real world via online visual language mapping. *arXiv preprint arXiv:2310.10822*, 2023. 1
- [89] Haofei Xu, Jing Zhang, Jianfei Cai, Hamid Rezaatofighi, and Dacheng Tao. Gmflow: Learning optical flow via global matching. In *Proceedings of the IEEE/CVF conference on computer vision and pattern recognition (CVPR)*, 2022. 3, 7
- [90] Karmesh Yadav, Arjun Majumdar, Ram Ramrakhya, Naoki Yokoyama, Alexei Baevski, Zsolt Kira, Oleksandr Maksymets, and Dhruv Batra. Ovrl-v2: A simple state-of-art baseline for imagenav and objectnav. *arXiv preprint arXiv:2303.07798*, 2023. 3
- [91] Karmesh Yadav, Ram Ramrakhya, Arjun Majumdar, Vincent-Pierre Berges, Sachit Kuhar, Dhruv Batra, Alexei Baevski, and Oleksandr Maksymets. Offline visual representation learning for embodied navigation. In *Workshop on Reincarnating Reinforcement Learning at ICLR 2023*, 2023. 1, 3
- [92] Weirui Ye, Yunsheng Zhang, Pieter Abbeel, and Yang Gao. Become a proficient player with limited data through watching pure videos. In *International Conference on Learning Representations (ICLR)*, 2022. 3
- [93] Jiazhao Zhang, Kunyu Wang, Rongtao Xu, Gengze Zhou, Yicong Hong, Xiaomeng Fang, Qi Wu, Zhizheng Zhang, and Wang He. Navid: Video-based vlm plans the next step for vision-and-language navigation. *arXiv preprint arXiv:2402.15852*, 2024. 3, 5
- [94] Jiazhao Zhang, Kunyu Wang, Rongtao Xu, Gengze Zhou, Yicong Hong, Xiaomeng Fang, Qi Wu, Zhizheng Zhang, and Wang He. Navid: Video-based vlm plans the next step for vision-and-language navigation. *arXiv preprint arXiv:2402.15852*, 2024. 3
- [95] Bolei Zhou, Agata Lapedriza, Aditya Khosla, Aude Oliva, and Antonio Torralba. Places: A 10 million image database for scene recognition. *IEEE Transactions on Pattern Analysis and Machine Intelligence (TPAMI)*, 2017. 4, 1
- [96] Bohan Zhou, Ke Li, Jiechuan Jiang, and Zongqing Lu. Learning from visual observation via offline pretrained state-to-go transformer. In *Neural Information Processing Systems (NeurIPS)*, 2024. 3
- [97] Xingyi Zhou, Rohit Girdhar, Armand Joulin, Philipp Krähenbühl, and Ishan Misra. Detecting twenty-thousand classes using image-level supervision. In *European Conference on Computer Vision (ECCV)*, 2022. 5
- [98] Deyao Zhu, Yuhui Wang, Jürgen Schmidhuber, and Mohamed Elhoseiny. Guiding online reinforcement learning with action-free offline pretraining. *arXiv preprint arXiv:2301.12876*, 2023. 3
- [99] Yuke Zhu, Roozbeh Mottaghi, Eric Kolve, Joseph J Lim, Abhinav Gupta, Li Fei-Fei, and Ali Farhadi. Target-driven visual navigation in indoor scenes using deep reinforcement learning. In *2017 IEEE international conference on robotics and automation (ICRA)*, 2017. 3

# NOLO: Navigate Only Look Once

## Supplementary Material

### 6. Methodology Details

#### 6.1. Pseudo Action Labeling

We deploy optical flow and filter dominant vectors with the help of the flow map. Theoretically, discretizing filtered vectors into several action categories can be achieved by any unsupervised pattern recognition methods, such as clustering. In practice, we use a simple threshold-based heuristic. We observe that the feature of moving forward is less prominent than turning left or right. Consequently, we focus more on the horizontal displacement of the pixels in the flow map. If the horizontal component of horizontal displacement exceeds a threshold  $\tau_x$  and the vertical component stays within a threshold  $\tau_y$  then we classify it as a turning action, or it is considered as a forwarding action.

Occasionally, we notice that the displacement of pixels observed across frames manifests irregular patterns. To mitigate this issue, for each pair of adjacent frames  $(f_t, f_{t+1})$ , we filter dominant vectors  $\nu_t$  that exhibit gradient amplitudes within the upper decile, which are subsequently discretized into actions derived from the action space, making it possible to trace the trajectory of the agent over time.

#### 6.2. Policy Inference

We choose the threshold of choosing action  $\beta = 0.5$ . After the loss of BCQ converges, we make decisions based on the learned policy and Q-values. During inference, an action is chosen based on the Q-values weighted by masked action distribution  $\pi_\theta(a_t|g, o_t, \mathcal{T}^i)$  with probability  $\varepsilon = 0.999$  and otherwise randomly. Besides, as long as  $P_D$  outputs a strong signal for termination, the agent will directly output action *STOP*.

#### 6.3. Semantic Actions

To ensure more stable navigation, the VN $\odot$ Bert is elaborately designed to output "semantic actions", i.e. actions from the action space along with their duration. For example, (MoveForward, 3) means repeatedly moving forward for 3 time steps. STOP can be executed at most once. We find that limiting each action up to 3 times at most effectively improves the robustness of the learned policy and the final performance. Previous methods [13, 34] tend to adopt a more complicated hierarchical framework consisting of a high-level policy to propose sub-goals from a constructed topological map and a low-level policy to decompose several actions in the action space to reach each sub-goal. Instead, we adopt a simpler but more practical mid-level policy to regularize the navigation behavior. From another perspective, we enlarge the original action space to an extended

one with 10 new actions.

#### 6.4. Model Architecture

We deploy ResNet18 pretrained from Places368 [95] as visual Encoder and frozen ResNet50-based Clip visual encoder as goal image encoder. In VN $\odot$ Bert, the self-attention modules consist of 9 Bert [21] layers and the cross-attention modules consist of 4 LXMERT [81] layers. The structure of VN $\odot$ Bert is modified from Prevalent [35]. The self-attention modules and cross-attention modules are also initialized with the checkpoints of Prevalent. Our codes and documents are included in supplementary materials.

### 7. Experiment Details

#### 7.1. Dataset Division

Derived from Ai2THOR, valid scenes in RoboTHOR are in the form FloorPlan\_Train{1:12}\_{-}{1:5} or FloorPlan\_Val{1:3}\_{-}{1:5}. See Tab. 3 for training and testing scene splits. We include detailed steps in the README.md contained in the supplementary materials indicating how to run scripts to create video datasets and gather testing points.

#### 7.2. LMM Baselines

For both GPT-4o and Video-LLaVA, we maintain a queue of size  $K = 16$  to incorporate sampled context frames, current observation, and goal image into a video clip and designed a consistent prompt to facilitate their understanding of the video content and to guide them to provide a reasonable action at each timestep. The prompt is structured as follows:

```
These frames pertain to a navigation task. The goal of the video is represented by the last frame, and the second-to-last frame is the current observation. Choose the best action from [move forward, turn left, turn right, stop] that will help achieve the goal depicted in the last frame of the video. Please provide the selected action directly.
```

We then utilize regular expressions to extract actions from the received language responses. In case of invalid output, we attempt up to three retries, and a random action is selected as output if all attempts fail.

Table 3. Dataset division of RoboTHOR and Habitat

Train		
S9hNv5qa7GM	XcA2TqTSSAj	PX4nDJXEHRG
5LpN3gDmAk7	WYY7iVyf5p8	5q7pvUzZiYa
VFuaQ6m2Qom	EDJbREhghzL	rPc6DW4iMge
2n8kARJN3HM	HxpKQynjfin	PuKPg4mmafe
759xd9YjKW5	aayBHfsNo7d	jtcxE69GiFV
B6ByNegPMKs	p5wJjkQkbXX	D7N2EKCX4Sj
1LXtFkjl3qL	YVUC4YcDtcY	YmJkqBEsHnH
7y3sRwLe3Va	r47D5H71a5s	vyrNrziPKCB
gxdoqLR6rwA	1pXnuDYAj8r	VLzqgDo317F
kEZ7cmS4wCh	sT4fr6TAbpF	ARNzJeq3xxb
Vvot9Ly1tCj	cV4RveZvu5T	VVfe2KiqLaN
jh4fc5c5qoQ	2t7WUuJeko7	D7G3Y4iRVNrh
uNbn9QFRL6hY	V2XKFyX4ASd	e9zR4mvMWw7
RPmz2sHmrrY	E9uDoFAP3SH	17DRP5sb8fy
JeFG25nYj2p	mJXqzFtmKg4	YFuZgdQ5vWj
ac26ZMwG7aT	JF19kD82Mey	Pm6F8kyY3z2
sKLMlPTheUy	wc2JMjhGNzB	dhjEzFoUFzH
82sE5b5pLXE	gZ6f7yhEvPG	8WUmhLawc2A
5ZKStnWn8Zo	pRbA3pwrk9	29hnd4uzFmX
GdvgFV5R1Z5	ULsKaCPVFJR	q9vSo1VnCiC
Uxmj2M2itWa	qoiz87JEwZ2	s8pcmisQ38h
ur6pFq6Qu1A	fzynW3qQPVF	ZMojNkEp431
r1Q1Z4BcV1o	b8cTxDM8gDG	i5noydfURQK
JmbYfDe2QKZ		
Eval		
2azQ1b91cZZ	x8F5xyUWY9e	QUCTc6BB5sX
Vt2qJdWjCF2	gTV8FGcVJC9	EU6Fwq7SyZv
zsNo4HB9uLZ	X7HyMhZNoso	yqstnuAEVhm
SN83YJsR3w2	pLe4wQe7qrG	8194nk5LbLH
Z6MFQCViBuw	pa4otMbVnkk	VzqfbhrpDEA
TbHJrupSAjP	oLBMNvg9in8	rqfALeAoiTq
UwV83HsGsw3	gYvKGZ5eRqb	

### 7.3. Hyperparameters

Tab. 4 outlines the hyperparameters for VN $\odot$ Bert training.

### 7.4. Computation Resources

For both RoboTHOR and Habitat, we train NOLO and all NOLO-variants on a single 40G A100 GPU for around 1 day. We evaluate NOLO across all created testing tasks (single thread) on a 24G Nvidia RTX 4090 Ti GPU for about 6 hours in RoboTHOR and 5 hours in Habitat.

### 8. Additional Visualizations

Sec. 8 compares the t-SNE visual embedding sequence of a context video in RoboTHOR between NOLO and NOLO-T.

Table 4. Hyperparameters for VN $\odot$ Bert Training

Hyperparameter	Value
Optimizer	AdamW
Learning Rate	1e-4
Betas	(0.9,0.95)
Weight Decay	0.1
Batch size	26
SA Layers	9
CA Layers	4
Action Embedding Dimension	256
Visual Embedding Dimension	512
Hidden State Dimension	768
BCQ Clip Threshold	0.5
Type of GPUs	A100 & Nvidia RTX 4090 Ti

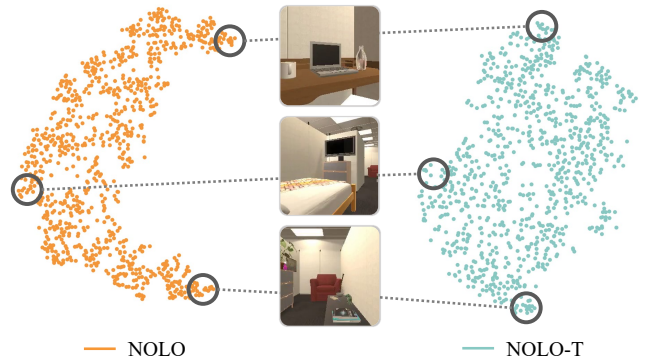


Figure 8. Comparison of context embedding sequences of a sampled video from RoboTHOR between NOLO and NOLO-T.

## 9. Evaluation Results

Tables below outline the average performance of different methods in RoboTHOR and Habitat as well as cross evaluation results over 3 random seeds.

### 9.1. RoboTHOR Evaluation Performance

We also examined the impact of NOLO compared to LMM baselines and visual navigation baselines on two key metrics for vision-based navigation tasks: Success Rate (SR) and Success weighted by normalized inverse Path Length (SPL), as illustrated in the figures in Fig. 9 and Fig. 10. Figs. 9a, 9b, 10a and 10b show the performance in the unseen layout testing set. Figs. 9c, 9d, 10c and 10d show the evaluation results in the unseen room testing set, and The detailed performances of NOLO, random policy, GPT-4o, Video-LLaVA, AVDC, VGM, ZSON, NOLO-C, NOLO-T, NOLO(M) in RoboTHOR are reported in Tabs. 5 to 14 respectively.

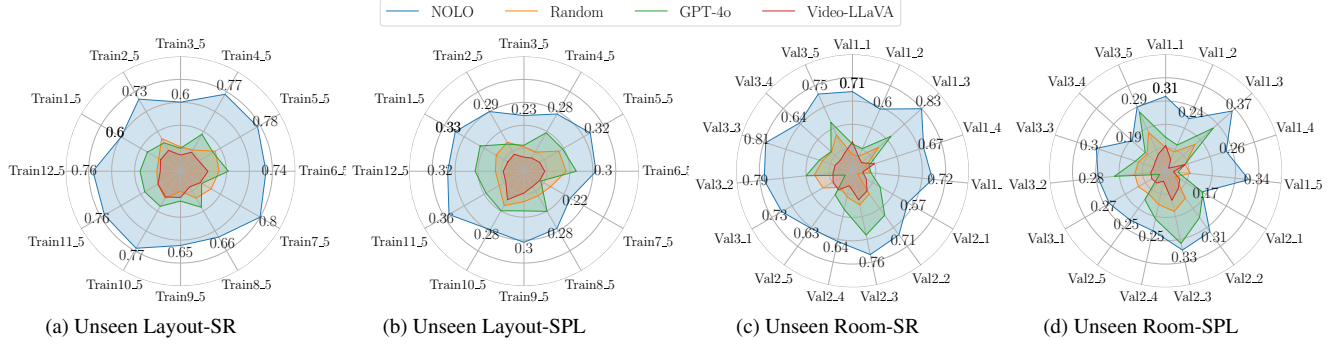


Figure 9. Compare NOLO with random policy and LMM baselines in RoboTHOR seen and unseen rooms.

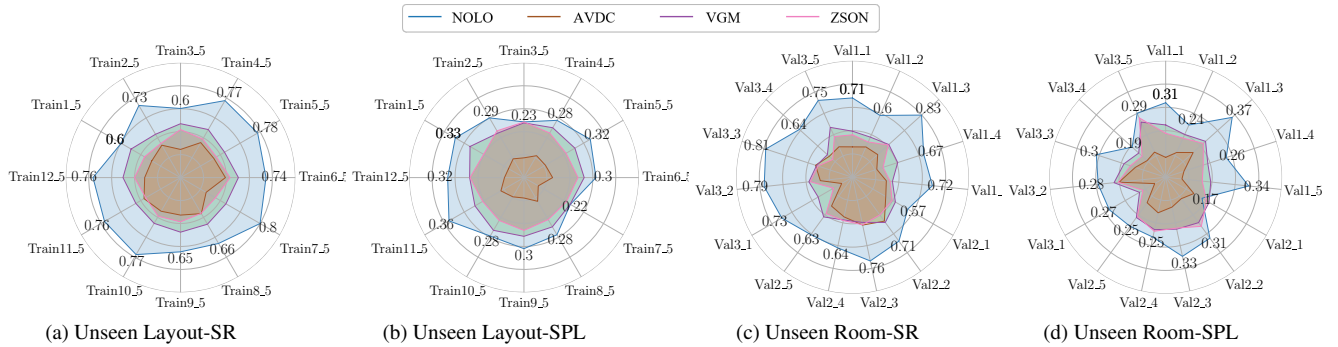


Figure 10. Compare NOLO with visual navigation baselines in RoboTHOR seen and unseen rooms.

## 9.2. Habitat Evaluation Performance

Also, we examined the impact of NOLO compared to LMM baselines and visual navigation baselines on two key metrics for vision-based navigation tasks: Success Rate (SR) and Success weighted by normalized inverse Path Length (SPL), as illustrated in Fig. 11. The performances of NOLO, random policy, GPT-4o, Video-LLaVA, AVDC, VGM, ZSON, NOLO-C, NOLO-T, NOLO(M) in Habitat testing scenes are reported in Tabs. 15 to 24 respectively.

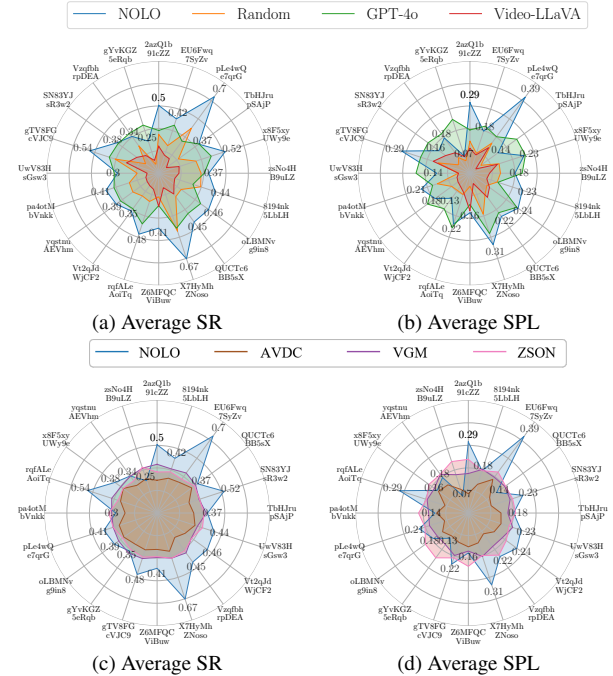


Figure 11. Compare NOLO with random policy, LMM baselines and visual navigation baselines in 20 Habitat testing scenes.

Table 5. NOLO performance on RoboTHOR testing set. “T” denotes FloorPlan\_Train and “V” denotes FloorPlan\_Val.

Scene	SR(%) $\uparrow$	SPL(%) $\uparrow$	TL $\downarrow$	NE $\downarrow$
T10_5	77.45 $\pm$ 4.36	28.21 $\pm$ 1.58	216.35 $\pm$ 14.21	1.68 $\pm$ 0.13
T11_5	76.44 $\pm$ 3.82	36.19 $\pm$ 2.32	218.66 $\pm$ 13.06	1.62 $\pm$ 0.16
T12_5	76.27 $\pm$ 3.54	31.89 $\pm$ 0.94	228.36 $\pm$ 4.96	1.50 $\pm$ 0.09
T1_5	59.72 $\pm$ 2.39	33.15 $\pm$ 1.72	260.69 $\pm$ 9.97	2.06 $\pm$ 0.05
T2_5	72.54 $\pm$ 0.81	28.83 $\pm$ 1.45	231.64 $\pm$ 4.56	1.76 $\pm$ 0.11
T3_5	60.20 $\pm$ 1.21	23.29 $\pm$ 0.21	289.70 $\pm$ 6.56	2.34 $\pm$ 0.04
T4_5	77.42 $\pm$ 2.74	27.64 $\pm$ 1.66	216.64 $\pm$ 6.83	1.71 $\pm$ 0.13
T5_5	77.58 $\pm$ 2.27	32.03 $\pm$ 1.45	227.46 $\pm$ 4.43	1.54 $\pm$ 0.09
T6_5	74.44 $\pm$ 4.37	30.13 $\pm$ 1.04	217.56 $\pm$ 6.36	1.90 $\pm$ 0.21
T7_5	80.00 $\pm$ 1.77	22.41 $\pm$ 1.20	239.99 $\pm$ 18.16	1.39 $\pm$ 0.11
T8_5	66.25 $\pm$ 8.84	27.60 $\pm$ 3.87	249.83 $\pm$ 31.73	2.07 $\pm$ 0.35
T9_5	64.67 $\pm$ 3.40	29.72 $\pm$ 1.78	270.19 $\pm$ 12.79	1.95 $\pm$ 0.11
Average	71.92	29.26	238.92	1.79
V1_1	70.83 $\pm$ 3.06	30.72 $\pm$ 0.78	241.85 $\pm$ 11.56	1.74 $\pm$ 0.17
V1_2	60.45 $\pm$ 3.04	23.57 $\pm$ 1.53	285.97 $\pm$ 5.54	2.31 $\pm$ 0.07
V1_3	82.98 $\pm$ 2.37	36.90 $\pm$ 2.38	178.16 $\pm$ 11.44	1.41 $\pm$ 0.11
V1_4	66.85 $\pm$ 2.05	26.25 $\pm$ 2.42	277.40 $\pm$ 15.40	1.85 $\pm$ 0.19
V1_5	71.81 $\pm$ 2.27	34.42 $\pm$ 0.91	238.96 $\pm$ 5.10	1.87 $\pm$ 0.12
V2_1	56.97 $\pm$ 2.61	17.31 $\pm$ 0.98	326.74 $\pm$ 9.13	2.30 $\pm$ 0.20
V2_2	70.56 $\pm$ 5.93	31.03 $\pm$ 1.34	241.85 $\pm$ 24.72	1.92 $\pm$ 0.17
V2_3	76.41 $\pm$ 3.16	33.33 $\pm$ 2.68	216.07 $\pm$ 8.19	1.49 $\pm$ 0.11
V2_4	64.36 $\pm$ 3.57	25.24 $\pm$ 0.84	263.61 $\pm$ 15.84	2.04 $\pm$ 0.15
V2_5	63.33 $\pm$ 3.02	24.99 $\pm$ 0.36	284.43 $\pm$ 5.26	2.44 $\pm$ 0.12
V3_1	72.86 $\pm$ 1.03	26.81 $\pm$ 2.75	240.61 $\pm$ 8.40	1.90 $\pm$ 0.07
V3_2	79.31 $\pm$ 4.62	27.97 $\pm$ 1.41	213.71 $\pm$ 14.15	1.60 $\pm$ 0.23
V3_3	81.48 $\pm$ 3.02	30.05 $\pm$ 1.48	213.88 $\pm$ 10.77	1.46 $\pm$ 0.08
V3_4	63.81 $\pm$ 5.10	18.56 $\pm$ 0.80	283.22 $\pm$ 10.86	2.11 $\pm$ 0.27
V3_5	75.14 $\pm$ 0.20	28.88 $\pm$ 2.25	220.18 $\pm$ 9.62	1.65 $\pm$ 0.04
Average	70.48	27.74	248.44	1.87

Table 6. Random performance on RoboTHOR testing set. “T” denotes FloorPlan\_Train and “V” denotes FloorPlan\_Val.

Scene	SR(%) $\uparrow$	SPL(%) $\uparrow$	TL $\downarrow$	NE $\downarrow$
T10_5	27.15 $\pm$ 0.50	16.55 $\pm$ 0.85	371.96 $\pm$ 3.07	2.84 $\pm$ 0.00
T11_5	22.83 $\pm$ 4.50	11.98 $\pm$ 2.67	406.66 $\pm$ 15.35	3.24 $\pm$ 0.22
T12_5	20.68 $\pm$ 1.26	11.93 $\pm$ 0.51	413.58 $\pm$ 4.25	3.02 $\pm$ 0.04
T1_5	22.00 $\pm$ 2.00	13.41 $\pm$ 1.47	396.63 $\pm$ 0.20	3.08 $\pm$ 0.09
T2_5	32.83 $\pm$ 0.93	14.00 $\pm$ 0.57	369.18 $\pm$ 2.40	2.54 $\pm$ 0.06
T3_5	21.26 $\pm$ 6.38	10.25 $\pm$ 0.81	421.76 $\pm$ 1.69	3.36 $\pm$ 0.09
T4_5	21.32 $\pm$ 2.23	9.23 $\pm$ 1.62	415.40 $\pm$ 9.71	3.08 $\pm$ 0.06
T5_5	34.95 $\pm$ 4.14	16.82 $\pm$ 1.57	373.65 $\pm$ 12.36	2.55 $\pm$ 0.16
T6_5	33.67 $\pm$ 2.00	17.65 $\pm$ 1.43	357.99 $\pm$ 0.93	2.76 $\pm$ 0.05
T7_5	30.75 $\pm$ 0.75	12.89 $\pm$ 0.42	391.34 $\pm$ 6.28	2.54 $\pm$ 0.12
T8_5	27.00 $\pm$ 1.75	11.85 $\pm$ 1.68	407.04 $\pm$ 8.17	3.16 $\pm$ 0.17
T9_5	17.50 $\pm$ 1.50	12.73 $\pm$ 0.25	412.05 $\pm$ 6.07	2.96 $\pm$ 0.02
Average	26.00	13.27	394.77	2.93
V1_1	14.50 $\pm$ 2.50	9.64 $\pm$ 0.75	436.59 $\pm$ 3.65	3.13 $\pm$ 0.22
V1_2	14.50 $\pm$ 4.50	8.63 $\pm$ 1.24	433.62 $\pm$ 8.48	3.25 $\pm$ 0.32
V1_3	31.61 $\pm$ 6.87	16.30 $\pm$ 0.77	382.54 $\pm$ 14.30	2.77 $\pm$ 0.13
V1_4	12.28 $\pm$ 3.28	8.49 $\pm$ 0.73	436.72 $\pm$ 9.52	3.18 $\pm$ 0.11
V1_5	16.17 $\pm$ 1.33	10.29 $\pm$ 0.50	424.95 $\pm$ 9.29	3.23 $\pm$ 0.12
V2_1	5.41 $\pm$ 3.68	4.71 $\pm$ 1.47	464.95 $\pm$ 11.81	3.17 $\pm$ 0.03
V2_2	25.61 $\pm$ 0.06	13.89 $\pm$ 0.33	395.96 $\pm$ 1.47	3.17 $\pm$ 0.12
V2_3	31.04 $\pm$ 2.04	17.05 $\pm$ 0.02	377.52 $\pm$ 5.43	2.17 $\pm$ 0.06
V2_4	23.73 $\pm$ 3.96	14.14 $\pm$ 0.76	398.90 $\pm$ 3.78	2.50 $\pm$ 0.10
V2_5	18.20 $\pm$ 1.37	11.74 $\pm$ 0.15	417.68 $\pm$ 0.58	3.25 $\pm$ 0.08
V3_1	30.45 $\pm$ 0.50	13.00 $\pm$ 0.84	381.07 $\pm$ 4.86	2.55 $\pm$ 0.01
V3_2	34.08 $\pm$ 1.75	12.83 $\pm$ 0.82	368.68 $\pm$ 1.57	2.79 $\pm$ 0.06
V3_3	28.39 $\pm$ 0.87	11.83 $\pm$ 0.51	394.93 $\pm$ 4.61	2.84 $\pm$ 0.05
V3_4	25.21 $\pm$ 3.83	10.30 $\pm$ 1.26	397.19 $\pm$ 9.02	3.01 $\pm$ 0.15
V3_5	35.33 $\pm$ 3.00	17.42 $\pm$ 1.22	376.74 $\pm$ 3.21	2.34 $\pm$ 0.07
Average	23.10	12.02	405.87	2.89

Table 7. GPT-4o performance on RoboTHOR testing set. “T” denotes FloorPlan\_Train and “V” denotes FloorPlan\_Val.

Scene	SR(%) $\uparrow$	SPL(%) $\uparrow$	TL $\downarrow$	NE $\downarrow$
T10_5	35.29	19.09	358.81	3.00
T11_5	36.00	18.32	363.55	3.15
T12_5	35.29	20.42	359.38	3.17
T1_5	33.33	21.14	362.02	2.78
T2_5	28.57	13.10	367.66	2.76
T3_5	20.00	10.86	377.68	3.30
T4_5	37.27	18.58	357.89	3.12
T5_5	32.73	18.66	363.37	2.95
T6_5	41.67	21.92	351.87	3.24
T7_5	21.25	8.14	374.45	3.10
T8_5	36.25	19.38	356.12	3.07
T9_5	26.00	16.57	366.02	2.72
Average	31.97	17.18	363.23	3.03
V1_1	24.00	13.84	374.19	3.45
V1_2	21.82	11.66	373.75	3.22
V1_3	46.32	26.44	342.01	2.53
V1_4	15.56	8.23	385.98	3.48
V1_5	16.59	5.07	390.28	3.10
V2_1	28.43	17.75	365.67	3.31
V2_2	48.95	23.77	346.67	2.09
V2_3	58.52	30.56	329.43	1.82
V2_4	35.23	20.31	360.92	2.09
V2_5	26.41	14.60	370.46	3.04
V3_1	7.48	2.94	391.37	4.18
V3_2	41.67	21.22	349.08	2.99
V3_3	31.11	13.08	369.33	2.73
V3_4	25.71	11.31	373.28	3.22
V3_5	47.50	26.64	346.99	2.09
Average	31.69	16.49	364.63	2.89

Table 8. Video-LLaVA performance on RoboTHOR testing set. “T” denotes FloorPlan\_Train and “V” denotes FloorPlan\_Val.

Scene	SR(%) $\uparrow$	SPL(%) $\uparrow$	TL $\downarrow$	NE $\downarrow$
T10_5	25.88	13.74	370.67	2.86
T11_5	22.67	8.79	380.99	3.58
T12_5	17.65	8.67	379.87	3.30
T1_5	20.00	7.78	383.98	2.77
T2_5	20.95	8.18	382.31	2.67
T3_5	14.12	5.89	388.76	3.84
T4_5	19.09	6.39	385.62	3.31
T5_5	18.18	7.55	385.68	3.04
T6_5	23.84	8.69	378.77	2.78
T7_5	19.86	7.67	382.04	3.01
T8_5	15.79	7.32	384.94	2.84
T9_5	22.83	9.11	379.34	2.98
Average	20.07	8.31	381.92	3.08
V1_1	25.92	10.42	374.65	3.01
V1_2	13.64	5.17	389.82	3.44
V1_3	10.92	1.66	396.36	3.65
V1_4	20.47	8.40	382.13	3.13
V1_5	9.17	3.28	395.26	3.63
V2_1	14.21	6.74	388.84	3.61
V2_2	22.12	8.90	377.86	3.30
V2_3	26.38	12.39	372.44	3.13
V2_4	13.53	4.34	391.22	4.01
V2_5	20.85	6.12	387.35	3.21
V3_1	20.00	6.59	381.67	2.93
V3_2	17.46	6.13	387.79	2.94
V3_3	16.29	5.24	388.70	2.91
V3_4	14.36	5.76	388.94	3.55
V3_5	17.38	7.51	382.77	3.34
Average	17.51	6.58	385.72	3.32

Table 9. AVDC performance on RoboTHOR testing set. T” denotes FloorPlan\_Train and V” denotes FloorPlan\_Val.

Scene	SR(%)↑	SPL(%)↑	TL↓	NE↓
T10_5	33.84	9.29	422.72	1.92
T11_5	36.72	11.13	434.58	2.22
T12_5	31.24	8.14	437.61	2.12
T1_5	28.98	7.44	428.73	2.00
T2_5	32.59	9.05	440.12	2.14
T3_5	24.53	8.26	444.36	2.45
T4_5	35.21	10.57	423.94	1.99
T5_5	33.47	10.36	433.51	2.09
T6_5	39.12	11.98	415.89	2.32
T7_5	25.74	6.92	439.82	2.18
T8_5	36.23	11.45	421.16	2.27
T9_5	32.67	8.54	426.75	2.15
Average	32.53	9.43	430.77	2.15
V1_1	27.14	8.21	462.48	2.65
V1_2	29.62	11.18	440.87	2.53
V1_3	30.28	15.24	405.27	1.84
V1_4	22.84	7.91	454.28	2.59
V1_5	30.41	6.76	447.91	2.21
V2_1	34.32	13.43	425.68	2.05
V2_2	48.45	10.92	398.67	1.25
V2_3	43.67	12.57	387.45	1.73
V2_4	36.18	14.97	404.22	1.49
V2_5	31.84	12.98	412.88	2.29
V3_1	11.14	5.23	450.75	3.07
V3_2	28.89	19.34	409.38	1.97
V3_3	34.67	13.15	429.52	2.21
V3_4	27.93	10.27	439.74	2.55
V3_5	29.78	11.33	399.28	1.53
Average	31.14	11.57	424.56	2.13

Table 10. VGM performance on RoboTHOR testing set. T” denotes FloorPlan\_Train and V” denotes FloorPlan\_Val.

Scene	SR(%)↑	SPL(%)↑	TL↓	NE↓
T10_5	46.02	25.47	375.88	2.49
T11_5	44.98	23.65	392.45	2.71
T12_5	50.13	22.71	378.29	2.39
T1_5	49.75	26.02	371.15	2.55
T2_5	43.59	21.54	388.67	2.23
T3_5	46.93	22.88	367.36	2.67
T4_5	48.32	24.07	381.74	2.41
T5_5	44.25	24.61	373.28	2.44
T6_5	50.41	25.19	369.24	2.33
T7_5	45.67	22.32	365.72	2.62
T8_5	46.89	23.78	380.91	2.35
T9_5	47.54	24.56	378.32	2.13
Average	47.04	23.90	376.92	2.44
V1_1	41.13	21.57	405.87	2.64
V1_2	39.23	19.31	412.88	2.87
V1_3	43.67	22.13	386.24	1.77
V1_4	42.45	18.27	416.54	2.41
V1_5	35.88	18.68	401.96	2.54
V2_1	44.26	20.67	382.33	2.38
V2_2	49.87	23.12	394.56	1.85
V2_3	41.22	21.87	385.19	1.91
V2_4	38.96	22.07	396.72	2.25
V2_5	43.78	20.52	405.33	2.64
V3_1	35.37	12.43	420.64	3.22
V3_2	39.16	21.38	389.33	2.42
V3_3	33.78	18.04	406.57	2.11
V3_4	30.15	14.92	416.38	2.82
V3_5	48.76	24.87	392.94	1.87
Average	40.51	19.99	400.90	2.38

Table 11. ZSON performance on RoboTHOR testing set. ‘‘T’’ denotes FloorPlan\_Train and ‘‘V’’ denotes FloorPlan\_Val.

Scene	SR(%) $\uparrow$	SPL(%) $\uparrow$	TL $\downarrow$	NE $\downarrow$
T10_5	38.89	20.69	350.67	2.23
T11_5	35.06	19.92	362.44	2.41
T12_5	40.06	22.54	345.23	2.16
T1_5	36.17	19.45	358.91	2.09
T2_5	34.37	22.58	351.12	2.02
T3_5	41.86	23.24	340.11	2.34
T4_5	38.72	21.52	346.72	2.29
T5_5	36.06	20.35	349.33	2.25
T6_5	43.17	22.61	335.84	2.38
T7_5	35.17	20.45	360.17	2.15
T8_5	35.96	20.27	348.52	2.31
T9_5	38.52	22.08	342.66	2.18
Average	37.83	21.31	349.31	2.23
V1_1	37.91	18.12	378.87	2.72
V1_2	34.50	17.64	386.19	2.91
V1_3	43.06	20.88	359.72	1.77
V1_4	28.71	16.29	395.18	2.56
V1_5	33.77	15.17	380.14	2.64
V2_1	40.93	19.42	361.48	2.12
V2_2	41.60	25.01	353.26	1.43
V2_3	43.34	21.41	368.11	1.85
V2_4	39.55	22.75	354.24	2.25
V2_5	40.02	19.83	360.73	2.72
V3_1	19.52	10.81	392.54	3.22
V3_2	37.89	19.64	368.18	2.56
V3_3	32.41	15.28	382.45	2.21
V3_4	23.77	13.04	390.76	2.89
V3_5	39.79	26.81	358.32	1.73
Average	35.78	18.81	372.68	2.37

Table 12. NOLO-C performance on RoboTHOR testing set. ‘‘T’’ denotes FloorPlan\_Train and ‘‘V’’ denotes FloorPlan\_Val.

Scene	SR(%) $\uparrow$	SPL(%) $\uparrow$	TL $\downarrow$	NE $\downarrow$
T10_5	72.94 $\pm$ 5.08	27.83 $\pm$ 0.15	252.83 $\pm$ 8.62	1.86 $\pm$ 0.29
T11_5	82.00 $\pm$ 1.44	36.28 $\pm$ 2.90	195.77 $\pm$ 8.38	1.50 $\pm$ 0.05
T12_5	73.53 $\pm$ 0.83	32.13 $\pm$ 1.26	230.53 $\pm$ 8.63	1.59 $\pm$ 0.05
T1_5	64.72 $\pm$ 1.04	32.41 $\pm$ 1.39	258.61 $\pm$ 2.70	1.94 $\pm$ 0.06
T2_5	70.63 $\pm$ 3.40	29.21 $\pm$ 3.18	243.38 $\pm$ 16.56	1.78 $\pm$ 0.11
T3_5	62.16 $\pm$ 1.94	23.55 $\pm$ 0.62	288.69 $\pm$ 8.45	2.27 $\pm$ 0.09
T4_5	72.12 $\pm$ 5.77	27.65 $\pm$ 0.21	244.76 $\pm$ 16.37	1.89 $\pm$ 0.20
T5_5	75.61 $\pm$ 0.57	32.77 $\pm$ 1.68	232.83 $\pm$ 3.66	1.60 $\pm$ 0.04
T6_5	67.78 $\pm$ 4.37	27.60 $\pm$ 0.31	254.15 $\pm$ 5.21	2.00 $\pm$ 0.12
T7_5	75.62 $\pm$ 1.84	19.90 $\pm$ 2.02	256.17 $\pm$ 8.42	1.55 $\pm$ 0.03
T8_5	65.62 $\pm$ 2.55	26.02 $\pm$ 2.55	253.82 $\pm$ 8.94	2.00 $\pm$ 0.07
T9_5	56.67 $\pm$ 4.11	24.40 $\pm$ 2.52	303.16 $\pm$ 8.15	2.18 $\pm$ 0.05
Average	69.95	28.31	251.23	1.85
V1_1	64.33 $\pm$ 5.44	25.29 $\pm$ 5.10	283.93 $\pm$ 29.92	2.12 $\pm$ 0.22
V1_2	57.42 $\pm$ 3.57	22.97 $\pm$ 1.36	305.57 $\pm$ 10.25	2.34 $\pm$ 0.15
V1_3	82.98 $\pm$ 1.38	41.56 $\pm$ 1.40	197.25 $\pm$ 10.54	1.43 $\pm$ 0.04
V1_4	62.22 $\pm$ 3.27	25.73 $\pm$ 1.58	284.70 $\pm$ 10.51	2.26 $\pm$ 0.10
V1_5	58.61 $\pm$ 1.42	31.95 $\pm$ 2.50	276.70 $\pm$ 4.67	2.53 $\pm$ 0.12
V2_1	52.73 $\pm$ 1.96	17.41 $\pm$ 1.69	336.15 $\pm$ 1.47	2.59 $\pm$ 0.08
V2_2	67.22 $\pm$ 4.33	28.52 $\pm$ 2.17	268.21 $\pm$ 2.39	1.95 $\pm$ 0.07
V2_3	79.74 $\pm$ 3.46	35.81 $\pm$ 0.85	209.43 $\pm$ 23.21	1.34 $\pm$ 0.08
V2_4	62.95 $\pm$ 6.01	25.65 $\pm$ 0.77	276.85 $\pm$ 16.89	2.10 $\pm$ 0.19
V2_5	58.70 $\pm$ 0.94	24.36 $\pm$ 1.83	290.25 $\pm$ 2.98	2.55 $\pm$ 0.05
V3_1	71.43 $\pm$ 2.33	26.32 $\pm$ 3.77	240.97 $\pm$ 20.02	2.00 $\pm$ 0.14
V3_2	71.53 $\pm$ 1.75	26.78 $\pm$ 0.32	238.58 $\pm$ 3.53	1.99 $\pm$ 0.09
V3_3	72.59 $\pm$ 4.57	27.82 $\pm$ 1.74	242.52 $\pm$ 9.40	1.73 $\pm$ 0.18
V3_4	57.30 $\pm$ 2.65	18.35 $\pm$ 0.51	300.88 $\pm$ 11.16	2.30 $\pm$ 0.08
V3_5	70.97 $\pm$ 3.16	29.52 $\pm$ 1.81	243.77 $\pm$ 19.50	1.96 $\pm$ 0.14
Average	66.05	27.20	266.38	2.08

Table 13. NOLO-T performance on RoboTHOR testing set. “T” denotes FloorPlan\_Train and “V” denotes FloorPlan\_Val.

Scene	SR(%) $\uparrow$	SPL(%) $\uparrow$	TL $\downarrow$	NE $\downarrow$
T10_5	76.47 $\pm$ 3.53	29.97 $\pm$ 2.31	225.76 $\pm$ 18.05	1.71 $\pm$ 0.16
T11_5	78.00 $\pm$ 0.67	36.00 $\pm$ 0.43	210.91 $\pm$ 7.94	1.56 $\pm$ 0.10
T12_5	75.88 $\pm$ 0.59	30.77 $\pm$ 1.29	233.25 $\pm$ 4.82	1.62 $\pm$ 0.02
T1_5	64.17 $\pm$ 2.50	32.47 $\pm$ 4.30	254.97 $\pm$ 6.37	2.07 $\pm$ 0.01
T2_5	65.71 $\pm$ 6.67	26.12 $\pm$ 4.84	259.38 $\pm$ 29.69	1.95 $\pm$ 0.25
T3_5	59.41 $\pm$ 4.12	22.67 $\pm$ 0.98	303.37 $\pm$ 11.79	2.39 $\pm$ 0.08
T4_5	72.73 $\pm$ 0.91	27.02 $\pm$ 2.10	238.05 $\pm$ 10.76	1.89 $\pm$ 0.09
T5_5	78.18 $\pm$ 3.64	33.88 $\pm$ 0.94	224.37 $\pm$ 22.06	1.48 $\pm$ 0.12
T6_5	74.17 $\pm$ 0.83	32.28 $\pm$ 1.91	216.92 $\pm$ 17.75	1.83 $\pm$ 0.11
T7_5	80.62 $\pm$ 0.62	23.85 $\pm$ 1.03	232.86 $\pm$ 15.75	1.38 $\pm$ 0.08
T8_5	66.25 $\pm$ 2.50	30.95 $\pm$ 2.62	245.14 $\pm$ 15.49	2.06 $\pm$ 0.12
T9_5	61.00 $\pm$ 1.00	28.92 $\pm$ 1.60	285.27 $\pm$ 2.75	1.80 $\pm$ 0.20
Average	71.05	29.57	244.19	1.81
V1_1	64.00 $\pm$ 2.00	26.54 $\pm$ 1.03	277.16 $\pm$ 12.08	2.25 $\pm$ 0.02
V1_2	64.55	25.30 $\pm$ 0.81	272.34 $\pm$ 12.70	2.20 $\pm$ 0.01
V1_3	80.53 $\pm$ 5.79	36.93 $\pm$ 0.98	201.32 $\pm$ 9.73	1.62 $\pm$ 0.22
V1_4	59.44 $\pm$ 7.22	25.50 $\pm$ 1.25	283.97 $\pm$ 24.48	2.14 $\pm$ 0.21
V1_5	62.50 $\pm$ 0.83	32.49 $\pm$ 0.23	268.84 $\pm$ 5.32	2.06 $\pm$ 0.01
V2_1	56.36 $\pm$ 0.91	17.59 $\pm$ 0.30	329.25 $\pm$ 10.75	2.44 $\pm$ 0.04
V2_2	65.56 $\pm$ 2.22	30.85 $\pm$ 2.09	256.13 $\pm$ 9.46	2.07 $\pm$ 0.07
V2_3	76.92 $\pm$ 1.54	34.22 $\pm$ 0.03	209.07 $\pm$ 4.52	1.59 $\pm$ 0.02
V2_4	68.08 $\pm$ 0.38	25.24 $\pm$ 0.19	265.69 $\pm$ 6.21	1.93 $\pm$ 0.00
V2_5	65.22 $\pm$ 3.48	24.79 $\pm$ 0.74	290.28 $\pm$ 11.04	2.29 $\pm$ 0.14
V3_1	69.52 $\pm$ 0.95	25.09 $\pm$ 0.17	244.60 $\pm$ 10.47	2.04 $\pm$ 0.03
V3_2	75.83 $\pm$ 0.83	27.14 $\pm$ 2.16	223.59 $\pm$ 6.15	1.81 $\pm$ 0.06
V3_3	73.70 $\pm$ 2.59	24.63 $\pm$ 2.77	245.72 $\pm$ 15.48	1.75 $\pm$ 0.15
V3_4	52.38 $\pm$ 3.81	17.61 $\pm$ 0.82	316.57 $\pm$ 4.58	2.46 $\pm$ 0.12
V3_5	76.67 $\pm$ 0.83	31.29 $\pm$ 1.91	211.91 $\pm$ 5.29	1.62 $\pm$ 0.04
Average	67.42	27.01	259.76	2.02

Table 14. NOLO(M) performance on RoboTHOR testing set. “T” denotes FloorPlan\_Train and “V” denotes FloorPlan\_Val.

Scene	SR(%) $\uparrow$	SPL(%) $\uparrow$	TL $\downarrow$	NE $\downarrow$
T10_5	80.59 $\pm$ 4.12	32.92 $\pm$ 1.93	202.68 $\pm$ 22.39	1.47 $\pm$ 0.12
T11_5	77.33 $\pm$ 2.67	36.00 $\pm$ 3.27	218.04 $\pm$ 1.64	1.64 $\pm$ 0.01
T12_5	78.82	36.62 $\pm$ 0.82	211.44 $\pm$ 9.89	1.55 $\pm$ 0.01
T1_5	50.83 $\pm$ 5.83	27.99 $\pm$ 2.85	302.14 $\pm$ 14.69	2.35 $\pm$ 0.10
T2_5	69.05 $\pm$ 1.43	25.09 $\pm$ 2.83	256.49 $\pm$ 1.55	1.85 $\pm$ 0.13
T3_5	54.71 $\pm$ 0.59	21.49 $\pm$ 0.94	312.69 $\pm$ 3.18	2.61 $\pm$ 0.08
T4_5	73.64 $\pm$ 2.73	25.06 $\pm$ 1.03	245.16 $\pm$ 17.39	1.78 $\pm$ 0.08
T5_5	75.45 $\pm$ 0.91	31.23 $\pm$ 1.14	234.16 $\pm$ 1.94	1.75 $\pm$ 0.07
T6_5	65.83 $\pm$ 2.50	24.81 $\pm$ 0.36	276.04 $\pm$ 19.72	1.95 $\pm$ 0.01
T7_5	70.62 $\pm$ 0.63	19.64 $\pm$ 0.81	281.29 $\pm$ 2.88	1.77 $\pm$ 0.05
T8_5	59.38 $\pm$ 6.87	23.84 $\pm$ 2.27	287.47 $\pm$ 17.78	2.38 $\pm$ 0.37
T9_5	59.00 $\pm$ 7.00	31.86 $\pm$ 5.95	278.41 $\pm$ 28.49	2.12 $\pm$ 0.22
Average	67.94	28.05	258.83	1.93
V1_1	60.00 $\pm$ 3.00	25.32 $\pm$ 3.23	294.85 $\pm$ 21.57	2.29 $\pm$ 0.09
V1_2	60.00 $\pm$ 1.82	24.32 $\pm$ 3.48	291.72 $\pm$ 6.24	2.18 $\pm$ 0.09
V1_3	82.63 $\pm$ 1.58	35.75 $\pm$ 3.13	200.15 $\pm$ 3.24	1.41 $\pm$ 0.09
V1_4	62.22 $\pm$ 1.11	24.95 $\pm$ 0.16	288.34 $\pm$ 6.13	2.19 $\pm$ 0.21
V1_5	64.58 $\pm$ 4.58	31.77 $\pm$ 3.05	265.98 $\pm$ 16.41	2.04 $\pm$ 0.16
V2_1	49.09 $\pm$ 1.82	14.51 $\pm$ 2.21	358.64 $\pm$ 2.52	2.68 $\pm$ 0.06
V2_2	66.11 $\pm$ 2.78	30.06 $\pm$ 1.07	261.83 $\pm$ 10.29	2.11 $\pm$ 0.15
V2_3	77.69 $\pm$ 0.77	31.33 $\pm$ 1.61	232.93 $\pm$ 6.27	1.49 $\pm$ 0.02
V2_4	57.69 $\pm$ 1.54	23.61 $\pm$ 0.69	296.56 $\pm$ 8.78	2.26 $\pm$ 0.07
V2_5	59.57 $\pm$ 4.78	23.29 $\pm$ 0.57	303.90 $\pm$ 19.02	2.48 $\pm$ 0.30
V3_1	70.48 $\pm$ 1.90	25.14 $\pm$ 1.24	254.00 $\pm$ 0.10	1.87 $\pm$ 0.06
V3_2	71.25 $\pm$ 0.42	25.59 $\pm$ 0.67	244.68 $\pm$ 2.23	1.88 $\pm$ 0.04
V3_3	67.78 $\pm$ 0.37	24.20 $\pm$ 1.78	258.00 $\pm$ 2.40	1.89 $\pm$ 0.03
V3_4	54.29 $\pm$ 0.95	13.15 $\pm$ 1.33	330.42 $\pm$ 8.02	2.40 $\pm$ 0.00
V3_5	67.50 $\pm$ 1.67	30.21 $\pm$ 4.40	246.60 $\pm$ 8.73	2.05 $\pm$ 0.04
Average	64.73	25.55	275.24	2.08

Table 15. NOLO performance in Habitat testing scenes.

Scene	SR(%) $\uparrow$	SPL(%) $\uparrow$	TL $\downarrow$	NE $\downarrow$
2azQ1b91cZZ	50.26 $\pm$ 3.10	28.99 $\pm$ 1.40	311.44 $\pm$ 11.24	2.80 $\pm$ 0.12
8194nk5LbLH	43.94 $\pm$ 1.55	22.60 $\pm$ 0.51	341.28 $\pm$ 1.28	3.10 $\pm$ 0.08
EU6Fwq7SyZv	42.33 $\pm$ 1.70	18.15 $\pm$ 1.13	362.99 $\pm$ 5.59	2.90 $\pm$ 0.06
QUCTc6BB5sX	44.67 $\pm$ 6.24	21.94 $\pm$ 1.36	344.75 $\pm$ 21.03	4.25 $\pm$ 0.84
SN83YJsR3w2	38.33 $\pm$ 6.24	15.74 $\pm$ 2.48	379.77 $\pm$ 17.81	2.97 $\pm$ 0.97
TbHJrupSAjP	36.67 $\pm$ 10.19	14.29 $\pm$ 3.23	376.57 $\pm$ 28.90	3.85 $\pm$ 0.79
UwV83HsGsw3	30.48 $\pm$ 3.75	13.66 $\pm$ 0.67	402.48 $\pm$ 14.42	4.80 $\pm$ 0.58
Vt2qJdWjCF2	34.58 $\pm$ 4.60	12.75 $\pm$ 4.26	387.33 $\pm$ 21.56	6.63 $\pm$ 0.81
VzqfbhrpDEA	33.70 $\pm$ 1.89	17.94 $\pm$ 1.15	377.91 $\pm$ 7.07	5.25 $\pm$ 0.22
X7HyMhZNoso	66.67 $\pm$ 4.38	30.84 $\pm$ 2.47	275.02 $\pm$ 20.74	1.37 $\pm$ 0.22
Z6MFQCViBuw	40.67 $\pm$ 6.18	16.25 $\pm$ 3.41	369.67 $\pm$ 21.35	4.62 $\pm$ 0.64
gTV8FGcVJC9	53.67 $\pm$ 4.03	29.49 $\pm$ 2.20	292.08 $\pm$ 12.03	3.98 $\pm$ 0.12
gYvKGZ5eRqb	25.00 $\pm$ 8.16	7.34 $\pm$ 4.04	433.63 $\pm$ 30.22	6.06 $\pm$ 0.59
oLBMNvg9in8	45.67 $\pm$ 4.03	24.45 $\pm$ 3.33	335.14 $\pm$ 14.15	2.19 $\pm$ 0.16
pLe4wQe7qrG	70.00 $\pm$ 2.72	38.63 $\pm$ 2.66	218.44 $\pm$ 6.09	0.88 $\pm$ 0.24
pa4otMbVnkk	41.11 $\pm$ 11.00	20.99 $\pm$ 6.68	346.89 $\pm$ 36.77	5.95 $\pm$ 1.17
rqfALeAoiTq	47.50 $\pm$ 3.12	21.92 $\pm$ 2.23	338.93 $\pm$ 11.95	2.57 $\pm$ 0.11
x8F5xyUWy9e	51.82 $\pm$ 0.74	23.36 $\pm$ 0.97	320.58 $\pm$ 4.80	2.91 $\pm$ 0.06
yqstnuAEVhm	38.89 $\pm$ 0.79	17.68 $\pm$ 1.86	369.21 $\pm$ 3.18	2.54 $\pm$ 0.12
zsNo4HB9uLZ	37.08 $\pm$ 3.28	18.48 $\pm$ 2.66	367.31 $\pm$ 11.94	3.77 $\pm$ 0.34
Average	43.65	20.77	347.57	3.67

Table 16. Random performance in Habitat testing scenes.

Scene	SR(%) $\uparrow$	SPL(%) $\uparrow$	TL $\downarrow$	NE $\downarrow$
2azQ1b91cZZ	28.73 $\pm$ 6.04	13.11 $\pm$ 3.30	386.34 $\pm$ 24.39	3.91 $\pm$ 0.26
8194nk5LbLH	32.68 $\pm$ 4.95	11.77 $\pm$ 0.59	380.37 $\pm$ 10.02	3.78 $\pm$ 0.13
EU6Fwq7SyZv	21.50 $\pm$ 2.50	8.57 $\pm$ 0.97	409.05 $\pm$ 12.59	5.07 $\pm$ 0.18
QUCTc6BB5sX	21.50 $\pm$ 0.50	10.60 $\pm$ 1.00	399.77 $\pm$ 3.10	5.67 $\pm$ 0.00
SN83YJsR3w2	12.00 $\pm$ 3.00	5.89 $\pm$ 1.05	428.02 $\pm$ 12.97	4.97 $\pm$ 0.14
TbHJrupSAjP	18.07 $\pm$ 0.21	5.57 $\pm$ 1.55	427.09 $\pm$ 10.29	5.89 $\pm$ 0.37
UwV83HsGsw3	15.93 $\pm$ 1.93	4.78 $\pm$ 1.42	435.46 $\pm$ 1.59	5.57 $\pm$ 0.16
Vt2qJdWjCF2	20.75 $\pm$ 1.75	8.75 $\pm$ 0.86	415.93 $\pm$ 1.07	6.02 $\pm$ 0.05
VzqfbhrpDEA	25.06 $\pm$ 2.28	7.90 $\pm$ 1.88	412.03 $\pm$ 12.59	5.14 $\pm$ 0.05
X7HyMhZNoso	45.21 $\pm$ 0.21	17.71 $\pm$ 0.35	342.76 $\pm$ 8.05	2.86 $\pm$ 0.03
Z6MFQCViBuw	17.50 $\pm$ 4.50	5.40 $\pm$ 1.41	430.17 $\pm$ 14.77	6.83 $\pm$ 0.48
gTV8FGcVJC9	34.00 $\pm$ 5.00	13.64 $\pm$ 1.80	370.20 $\pm$ 16.76	4.76 $\pm$ 0.08
gYvKGZ5eRqb	7.00 $\pm$ 3.00	5.39 $\pm$ 2.65	457.60 $\pm$ 20.20	7.21 $\pm$ 0.10
oLBMNvg9in8	20.50 $\pm$ 0.50	8.57 $\pm$ 1.53	418.56 $\pm$ 8.32	4.28 $\pm$ 0.10
pLe4wQe7qrG	41.17 $\pm$ 7.17	15.29 $\pm$ 4.11	348.37 $\pm$ 24.83	3.17 $\pm$ 0.90
pa4otMbVnkk	22.83 $\pm$ 7.83	14.06 $\pm$ 0.92	391.77 $\pm$ 29.37	6.59 $\pm$ 0.03
rqfALeAoiTq	22.00 $\pm$ 1.33	9.19 $\pm$ 2.09	410.70 $\pm$ 6.22	4.25 $\pm$ 0.36
x8F5xyUWy9e	29.05 $\pm$ 3.23	12.57 $\pm$ 0.77	388.25 $\pm$ 1.57	4.69 $\pm$ 0.14
yqstnuAEVhm	23.67 $\pm$ 1.17	9.23 $\pm$ 0.06	410.58 $\pm$ 9.25	3.90 $\pm$ 0.13
zsNo4HB9uLZ	31.37 $\pm$ 1.13	12.54 $\pm$ 0.88	377.44 $\pm$ 10.84	4.78 $\pm$ 0.14
Average	24.53	10.03	402.02	4.97

Table 17. GPT-4o performance in Habitat testing scenes.

Scene	SR(%) $\uparrow$	SPL(%) $\uparrow$	TL $\downarrow$	NE $\downarrow$
2azQ1b91cZZ	31.67	17.77	348.79	4.19
8194nk5LbLH	26.67	12.07	360.59	4.21
EU6Fwq7SyZv	37.41	20.31	347.59	5.10
QUCTc6BB5sX	36.90	20.04	347.43	6.38
SN83YJsR3w2	37.24	21.26	344.79	4.69
TbHJrupSAjP	36.89	23.76	339.05	2.99
UwV83HsGsw3	32.86	22.14	344.40	4.97
Vt2qJdWjCF2	32.50	18.00	350.69	7.19
VzqfbhrpDEA	36.67	19.97	346.93	5.26
X7HyMhZNoso	42.86	26.08	335.63	2.66
Z6MFQCViBuw	24.00	12.83	362.88	7.99
gTV8FGcVJC9	38.49	21.29	344.03	4.25
gYvKGZ5eRqb	37.46	23.24	340.84	4.58
oLBMNvg9in8	38.34	23.79	335.41	2.06
pLe4wQe7qrG	29.32	18.54	350.50	5.77
pa4otMbVnkk	34.82	16.11	351.36	5.98
rqfALeAoiTq	39.49	23.56	339.48	3.32
x8F5xyUWy9e	40.91	23.94	338.39	4.23
yqstnuAEVhm	35.00	21.56	345.06	3.41
zsNo4HB9uLZ	33.75	21.45	342.88	4.72
Average	35.16	20.39	345.84	4.70

Table 18. Video-LLaVA performance in Habitat testing scenes.

Scene	SR(%) $\uparrow$	SPL(%) $\uparrow$	TL $\downarrow$	NE $\downarrow$
2azQ1b91cZZ	20.00	10.21	381.51	3.77
8194nk5LbLH	12.50	7.28	387.78	5.17
EU6Fwq7SyZv	14.00	7.92	385.03	4.04
QUCTc6BB5sX	19.00	12.24	378.96	5.26
SN83YJsR3w2	20.00	12.34	379.00	3.72
TbHJrupSAjP	7.14	3.01	395.36	5.05
UwV83HsGsw3	8.57	4.70	393.87	5.29
Vt2qJdWjCF2	11.32	6.66	388.67	6.24
VzqfbhrpDEA	16.20	10.37	384.72	5.42
X7HyMhZNoso	11.27	4.48	393.52	4.49
Z6MFQCViBuw	24.60	15.43	371.56	4.64
gTV8FGcVJC9	25.00	15.86	371.61	4.50
gYvKGZ5eRqb	10.00	7.19	389.55	5.23
oLBMNvg9in8	14.00	9.90	380.34	4.40
pLe4wQe7qrG	13.33	12.94	377.50	3.17
pa4otMbVnkk	10.00	5.57	387.50	6.02
rqfALeAoiTq	12.50	8.34	386.06	3.91
x8F5xyUWy9e	15.91	11.81	380.44	3.43
yqstnuAEVhm	10.54	6.06	390.36	5.19
zsNo4HB9uLZ	15.01	8.03	387.20	5.30
Average	14.55	9.02	384.53	4.71

Table 19. AVDC performance in Habitat testing scenes.

Scene	SR(%)↑	SPL(%)↑	TL↓	NE↓
2azQ1b91cZZ	24.12	7.93	429.30	3.44
8194nk5LbLH	29.33	14.02	375.06	5.05
EU6Fwq7SyZv	26.95	12.35	442.17	5.45
QUCTc6BB5sX	22.14	10.48	450.81	3.54
SN83YJsR3w2	30.77	15.06	395.85	4.21
TbHJrupSAjP	31.49	10.74	420.21	4.96
UwV83HsGsw3	23.57	12.84	393.14	3.33
Vt2qJdWjCF2	28.05	11.54	426.06	4.42
VzqfbhrpDEA	25.22	14.19	410.55	3.45
X7HyMhZNoso	29.58	12.82	414.27	4.20
Z6MFQCViBuw	26.78	13.78	430.31	4.63
gTV8FGcVJC9	28.29	10.00	411.56	4.27
gYvKGZ5eRqb	26.52	10.18	421.96	4.92
oLBMNvg9in8	25.44	13.00	417.07	3.91
pLe4wQe7qrG	27.88	16.95	429.00	4.40
pa4otMbVnkk	29.31	10.21	434.91	5.12
rqfALeAoiTq	28.45	12.56	403.33	4.42
x8F5xyUWy9e	24.68	9.76	432.66	3.68
yqstnuAEVhm	30.19	13.00	399.91	4.39
zsNo4HB9uLZ	26.94	13.32	424.30	4.14
Average	27.29	12.24	418.12	4.30

Table 20. VGM performance in Habitat testing scenes.

Scene	SR(%)↑	SPL(%)↑	TL↓	NE↓
2azQ1b91cZZ	35.88	16.12	373.11	4.48
8194nk5LbLH	31.27	19.02	423.51	3.85
EU6Fwq7SyZv	34.10	18.74	368.62	4.06
QUCTc6BB5sX	36.27	16.88	367.95	4.29
SN83YJsR3w2	32.92	17.09	426.29	4.73
TbHJrupSAjP	35.08	18.43	395.03	4.40
UwV83HsGsw3	33.45	16.21	424.39	3.82
Vt2qJdWjCF2	36.12	15.91	403.36	4.64
VzqfbhrpDEA	33.57	19.50	397.14	3.67
X7HyMhZNoso	34.88	18.62	398.75	4.05
Z6MFQCViBuw	32.67	15.53	398.10	4.37
gTV8FGcVJC9	35.13	17.68	390.74	4.36
gYvKGZ5eRqb	34.77	16.44	393.34	4.36
oLBMNvg9in8	31.22	17.13	391.16	3.38
pLe4wQe7qrG	36.45	18.04	357.49	4.19
pa4otMbVnkk	34.02	16.66	414.59	3.99
rqfALeAoiTq	35.23	18.21	369.25	4.20
x8F5xyUWy9e	32.45	17.90	380.19	4.32
yqstnuAEVhm	34.99	15.80	412.49	4.17
zsNo4HB9uLZ	36.23	16.09	392.92	4.39
Average	34.34	17.30	393.92	4.19

Table 21. ZSON performance in Habitat testing scenes.

Scene	SR(%)↑	SPL(%)↑	TL↓	NE↓
2azQ1b91cZZ	30.22	21.90	400.05	4.49
8194nk5LbLH	35.14	17.42	397.11	4.13
EU6Fwq7SyZv	31.88	18.15	360.23	4.71
QUCTc6BB5sX	34.62	21.22	379.75	4.42
SN83YJsR3w2	30.87	19.88	415.70	4.21
TbHJrupSAjP	33.94	18.75	428.33	4.05
UwV83HsGsw3	35.56	20.32	391.88	3.92
Vt2qJdWjCF2	33.18	22.58	400.38	4.37
VzqfbhrpDEA	29.34	19.49	393.52	4.72
X7HyMhZNoso	34.90	18.22	376.97	4.29
Z6MFQCViBuw	32.12	21.74	380.55	4.91
gTV8FGcVJC9	30.25	17.96	406.00	4.35
gYvKGZ5eRqb	35.44	22.08	412.43	3.81
oLBMNvg9in8	31.53	19.14	366.82	4.58
pLe4wQe7qrG	30.87	20.69	393.75	4.14
pa4otMbVnkk	33.97	18.56	418.57	4.28
rqfALeAoiTq	34.12	19.24	378.22	4.33
x8F5xyUWy9e	32.78	18.97	416.39	3.91
yqstnuAEVhm	31.41	21.66	419.74	4.27
zsNo4HB9uLZ	34.55	19.31	382.41	4.43
Average	32.83	19.86	395.94	4.32

Table 22. NOLO-C performance in Habitat testing scenes.

Scene	SR(%)↑	SPL(%)↑	TL↓	NE↓
2azQ1b91cZZ	37.18± 4.28	22.84± 3.63	359.71± 17.26	4.38± 0.69
8194nk5LbLH	36.97± 1.55	19.47± 0.99	366.57± 4.66	2.97± 0.34
EU6Fwq7SyZv	34.00± 2.16	18.48± 0.86	378.66± 2.54	3.18± 0.31
QUCTc6BB5sX	40.33± 1.25	23.52± 0.77	355.46± 1.65	4.83± 0.32
SN83YJsR3w2	15.00± 7.07	6.92± 2.91	455.47± 15.62	4.56± 1.16
TbHJrupSAjP	20.95± 5.99	6.05± 1.97	437.43± 14.11	4.53± 0.51
UwV83HsGsw3	26.67± 1.35	17.00± 1.76	401.74± 3.26	4.77± 0.41
Vt2qJdWjCF2	19.17± 5.62	8.34± 0.78	437.86± 13.29	11.49± 0.85
VzqfbhrpDEA	25.19± 1.05	15.50± 2.16	398.60± 9.64	5.91± 1.16
X7HyMhZNoso	59.05± 2.94	30.08± 0.75	290.51± 7.25	2.00± 0.27
Z6MFQCViBuw	38.00± 5.66	15.43± 1.57	375.89± 16.03	5.19± 0.22
gTV8FGcVJC9	41.33± 1.70	25.04± 1.93	335.27± 13.56	4.63± 0.73
gYvKGZ5eRqb	11.67± 2.36	3.51± 1.45	474.47± 10.70	10.91± 0.46
oLBMNvg9in8	44.33± 2.36	25.58± 1.67	332.98± 8.66	1.85± 0.12
pLe4wQe7qrG	52.22± 3.14	26.99± 1.25	316.10± 10.12	1.54± 0.48
pa4otMbVnkk	14.44± 5.67	7.67± 3.04	447.38± 20.68	7.15± 1.53
rqfALeAoiTq	36.94± 4.63	18.40± 1.58	370.27± 11.73	2.45± 0.07
x8F5xyUWy9e	46.97± 4.71	21.66± 1.96	335.51± 11.35	2.43± 0.57
yqstnuAEVhm	38.61± 6.17	17.60± 3.23	372.49± 22.68	2.89± 0.55
zsNo4HB9uLZ	32.50± 3.54	18.14± 0.90	382.85± 11.49	3.92± 0.54
Average	33.58	17.41	381.26	4.58

Table 23. NOLO-T performance in Habitat testing scenes.

Scene	SR(%) $\uparrow$	SPL(%) $\uparrow$	TL $\downarrow$	NE $\downarrow$
2azQ1b91cZZ	41.28 $\pm$ 2.97	25.50 $\pm$ 2.75	344.03 $\pm$ 15.14	4.45 $\pm$ 0.08
8194nk5LbLH	39.70 $\pm$ 2.61	19.67 $\pm$ 0.74	364.86 $\pm$ 3.70	3.04 $\pm$ 0.27
EU6Fwq7SyZv	41.00 $\pm$ 3.27	21.33 $\pm$ 2.90	357.03 $\pm$ 11.76	3.37 $\pm$ 0.17
QUCTc6BB5sX	41.50 $\pm$ 4.50	21.52 $\pm$ 2.39	357.77 $\pm$ 11.40	5.51 $\pm$ 0.73
SN83YJsR3w2	21.67 $\pm$ 11.79	7.83 $\pm$ 4.20	432.92 $\pm$ 32.98	5.79 $\pm$ 1.89
TbHJrupSAjP	29.52 $\pm$ 0.67	11.53 $\pm$ 0.91	400.50 $\pm$ 5.36	4.45 $\pm$ 0.39
UwV83HsGsw3	28.10 $\pm$ 0.67	15.16 $\pm$ 2.66	398.37 $\pm$ 9.11	4.95 $\pm$ 0.19
Vt2qJdWjCF2	18.33 $\pm$ 3.12	7.74 $\pm$ 1.46	443.81 $\pm$ 10.96	11.66 $\pm$ 0.67
VzqfbhrpDEA	30.00 $\pm$ 0.91	16.90 $\pm$ 0.92	387.73 $\pm$ 5.64	7.28 $\pm$ 0.43
X7HyMhZNoso	63.33 $\pm$ 0.89	32.24 $\pm$ 0.69	270.01 $\pm$ 2.15	2.31 $\pm$ 0.39
Z6MFQCViBuw	40.67 $\pm$ 3.40	15.79 $\pm$ 3.40	380.14 $\pm$ 11.92	4.87 $\pm$ 0.44
gTV8FGcVJC9	46.50 $\pm$ 1.50	28.97 $\pm$ 1.96	313.77 $\pm$ 0.72	5.54 $\pm$ 0.94
gYvKGZ5eRqb	10.00	2.73 $\pm$ 0.50	471.45 $\pm$ 3.05	9.34 $\pm$ 1.00
oLBMNvg9in8	47.00 $\pm$ 1.00	24.69 $\pm$ 1.35	332.24 $\pm$ 4.97	1.92 $\pm$ 0.16
pLe4wQe7qrG	65.00 $\pm$ 1.67	28.04 $\pm$ 5.24	290.87 $\pm$ 27.90	0.58 $\pm$ 0.09
pa4otMbVnkk	33.33 $\pm$ 3.33	18.79 $\pm$ 0.48	365.55 $\pm$ 13.95	7.17 $\pm$ 0.66
rqfALeAoiTq	43.89 $\pm$ 2.19	22.01 $\pm$ 1.75	348.34 $\pm$ 8.51	2.55 $\pm$ 0.29
x8F5xyUWy9e	52.42 $\pm$ 0.43	22.44 $\pm$ 0.94	328.36 $\pm$ 2.28	2.13 $\pm$ 0.02
yqstnuAEVhm	38.61 $\pm$ 3.14	17.06 $\pm$ 2.82	372.31 $\pm$ 14.27	2.83 $\pm$ 0.13
zsNo4HB9uLZ	26.67 $\pm$ 1.18	16.10 $\pm$ 1.78	400.21 $\pm$ 5.77	4.74 $\pm$ 0.08
Average	37.93	18.80	368.01	4.72

Table 24. NOLO(M) performance in Habitat testing scenes.

Scene	SR(%) $\uparrow$	SPL(%) $\uparrow$	TL $\downarrow$	NE $\downarrow$
2azQ1b91cZZ	35.77 $\pm$ 0.38	21.70 $\pm$ 0.98	367.77 $\pm$ 0.44	5.26 $\pm$ 0.06
8194nk5LbLH	38.18 $\pm$ 0.91	19.20 $\pm$ 0.74	365.92 $\pm$ 3.05	3.05 $\pm$ 0.18
EU6Fwq7SyZv	40.50 $\pm$ 4.50	20.97 $\pm$ 1.42	360.27 $\pm$ 14.82	3.04 $\pm$ 0.49
QUCTc6BB5sX	40.00	22.11 $\pm$ 1.36	354.65 $\pm$ 1.51	4.64 $\pm$ 0.25
SN83YJsR3w2	32.50 $\pm$ 7.50	10.28 $\pm$ 2.55	414.92 $\pm$ 23.22	4.92 $\pm$ 1.20
TbHJrupSAjP	24.29 $\pm$ 1.43	7.48 $\pm$ 0.50	427.30 $\pm$ 6.51	4.63 $\pm$ 0.07
UwV83HsGsw3	30.71 $\pm$ 2.14	17.89 $\pm$ 3.05	390.06 $\pm$ 15.81	4.03 $\pm$ 0.21
Vt2qJdWjCF2	13.75 $\pm$ 1.25	6.65 $\pm$ 0.62	454.84 $\pm$ 0.97	12.59 $\pm$ 0.18
VzqfbhrpDEA	28.33 $\pm$ 3.89	14.89 $\pm$ 2.38	402.32 $\pm$ 9.62	7.08 $\pm$ 0.47
X7HyMhZNoso	64.64 $\pm$ 1.79	30.95 $\pm$ 0.11	276.48 $\pm$ 5.50	1.94 $\pm$ 0.15
Z6MFQCViBuw	37.00 $\pm$ 7.00	16.86 $\pm$ 3.37	374.19 $\pm$ 22.49	4.90 $\pm$ 0.33
gTV8FGcVJC9	50.50 $\pm$ 7.50	28.67 $\pm$ 1.23	306.25 $\pm$ 9.88	4.54 $\pm$ 0.72
gYvKGZ5eRqb	12.50 $\pm$ 2.50	3.79 $\pm$ 1.73	475.62 $\pm$ 14.77	9.55 $\pm$ 1.20
oLBMNvg9in8	48.00 $\pm$ 2.00	28.67 $\pm$ 0.73	319.90 $\pm$ 6.13	1.61 $\pm$ 0.16
pLe4wQe7qrG	53.33 $\pm$ 3.33	26.82 $\pm$ 1.01	311.75 $\pm$ 0.38	1.26 $\pm$ 0.19
pa4otMbVnkk	20.00	8.13 $\pm$ 0.40	431.58 $\pm$ 1.42	8.87 $\pm$ 0.33
rqfALeAoiTq	45.42 $\pm$ 2.08	20.42 $\pm$ 2.06	352.25 $\pm$ 7.54	2.19 $\pm$ 0.23
x8F5xyUWy9e	49.55 $\pm$ 4.09	22.50 $\pm$ 1.80	331.82 $\pm$ 12.30	2.14 $\pm$ 0.47
yqstnuAEVhm	42.08 $\pm$ 4.58	18.98 $\pm$ 3.12	360.02 $\pm$ 16.95	2.89 $\pm$ 0.05
zsNo4HB9uLZ	27.50	16.36 $\pm$ 1.47	400.51 $\pm$ 1.49	4.76 $\pm$ 0.10
Average	36.73	18.17	373.92	4.69

### 9.3. Cross Evaluation Results

The performances of H2R and R2H are reported in Tabs. 25 and 26 respectively.

Table 25. NOLO performance in RoboTHOR after training in Habitat. “T” denotes FloorPlan.Train and “V” denotes FloorPlan.Val.

Scene	SR(%) $\uparrow$	SPL(%) $\uparrow$	NE $\downarrow$	TL $\downarrow$
T10_5	60.00 $\pm$ 0.96	26.63 $\pm$ 1.37	303.93 $\pm$ 7.01	2.30 $\pm$ 0.13
T11_5	64.89 $\pm$ 3.50	31.85 $\pm$ 3.64	286.70 $\pm$ 20.00	2.09 $\pm$ 0.22
T12_5	52.16 $\pm$ 5.79	26.13 $\pm$ 3.37	326.15 $\pm$ 15.30	2.36 $\pm$ 0.24
T1_5	50.00 $\pm$ 6.24	29.40 $\pm$ 1.07	320.91 $\pm$ 10.47	2.46 $\pm$ 0.04
T2_5	47.94 $\pm$ 4.56	20.57 $\pm$ 4.91	339.62 $\pm$ 26.92	2.42 $\pm$ 0.18
T3_5	39.22 $\pm$ 3.09	18.48 $\pm$ 0.60	377.95 $\pm$ 6.26	3.30 $\pm$ 0.22
T4_5	64.24 $\pm$ 1.87	30.56 $\pm$ 0.79	279.33 $\pm$ 3.76	2.13 $\pm$ 0.13
T5_5	61.52 $\pm$ 0.86	27.48 $\pm$ 2.16	305.47 $\pm$ 7.33	2.06 $\pm$ 0.11
T6_5	60.56 $\pm$ 2.83	31.06 $\pm$ 4.18	285.57 $\pm$ 25.83	2.30 $\pm$ 0.16
T7_5	50.83 $\pm$ 0.59	20.54 $\pm$ 1.48	334.78 $\pm$ 0.93	2.30 $\pm$ 0.17
T8_5	54.58 $\pm$ 4.12	28.68 $\pm$ 1.69	297.57 $\pm$ 10.62	2.41 $\pm$ 0.02
T9_5	38.67 $\pm$ 6.60	22.46 $\pm$ 4.39	364.06 $\pm$ 18.55	2.53 $\pm$ 0.15
Average	53.72	26.15	318.50	2.39
V1_1	54.00 $\pm$ 4.32	28.45 $\pm$ 3.73	316.52 $\pm$ 19.28	2.34 $\pm$ 0.15
V1_2	48.48 $\pm$ 4.09	23.46 $\pm$ 3.96	338.57 $\pm$ 19.55	2.61 $\pm$ 0.12
V1_3	74.04 $\pm$ 4.06	39.60 $\pm$ 2.33	235.18 $\pm$ 8.91	1.71 $\pm$ 0.09
V1_4	44.07 $\pm$ 5.83	23.73 $\pm$ 1.69	350.40 $\pm$ 17.36	2.65 $\pm$ 0.12
V1_5	49.44 $\pm$ 4.10	27.90 $\pm$ 4.66	324.46 $\pm$ 26.83	2.68 $\pm$ 0.17
V2_1	32.73 $\pm$ 3.71	14.01 $\pm$ 1.79	404.18 $\pm$ 12.65	3.19 $\pm$ 0.10
V2_2	48.89 $\pm$ 0.91	24.29 $\pm$ 3.87	338.47 $\pm$ 12.65	2.96 $\pm$ 0.19
V2_3	67.18 $\pm$ 1.92	35.17 $\pm$ 2.13	278.73 $\pm$ 10.96	1.63 $\pm$ 0.08
V2_4	52.69 $\pm$ 0.38	25.33 $\pm$ 0.32	340.45 $\pm$ 7.34	2.33 $\pm$ 0.03
V2_5	44.35 $\pm$ 2.61	22.94 $\pm$ 1.82	353.16 $\pm$ 22.72	2.94 $\pm$ 0.11
V3_1	59.05 $\pm$ 2.86	29.58 $\pm$ 2.96	279.42 $\pm$ 18.76	2.24 $\pm$ 0.23
V3_2	56.39 $\pm$ 1.71	22.96 $\pm$ 1.40	310.36 $\pm$ 17.14	2.40 $\pm$ 0.08
V3_3	59.51 $\pm$ 4.58	26.33 $\pm$ 3.53	297.91 $\pm$ 19.58	2.22 $\pm$ 0.14
V3_4	41.59 $\pm$ 1.19	15.47 $\pm$ 1.16	360.06 $\pm$ 9.11	2.95 $\pm$ 0.01
V3_5	60.00 $\pm$ 2.36	27.78 $\pm$ 2.98	298.36 $\pm$ 11.92	2.15 $\pm$ 0.15
Average	52.83	25.80	321.75	2.47

Table 26. NOLO Performance in Habitat testing scenes after training in RoboTHOR.

Scene	SR(%) $\uparrow$	SPL(%) $\uparrow$	NE $\downarrow$	TL $\downarrow$
2azQ1b91cZZ	38.21 $\pm$ 0.96	23.38 $\pm$ 0.54	355.25 $\pm$ 4.81	6.45 $\pm$ 0.16
8194nk5LbLH	41.82 $\pm$ 2.23	21.25 $\pm$ 0.96	351.39 $\pm$ 6.97	4.85 $\pm$ 0.14
EU6Fwq7SyZv	45.67 $\pm$ 2.87	22.27 $\pm$ 1.75	345.99 $\pm$ 10.11	4.72 $\pm$ 0.37
QUCTc6BB5sX	44.00 $\pm$ 2.45	23.97 $\pm$ 1.79	346.11 $\pm$ 11.27	6.91 $\pm$ 0.19
SN83YJsR3w2	18.33 $\pm$ 4.71	7.28 $\pm$ 0.33	449.10 $\pm$ 9.22	9.20 $\pm$ 0.77
TbHJrupSAjP	28.10 $\pm$ 2.94	8.99 $\pm$ 0.80	422.23 $\pm$ 3.90	6.39 $\pm$ 0.26
UwV83HsGsw3	27.62 $\pm$ 4.10	14.83 $\pm$ 3.12	408.73 $\pm$ 7.70	7.07 $\pm$ 0.60
Vt2qJdWjCF2	17.92 $\pm$ 2.12	8.39 $\pm$ 1.65	436.55 $\pm$ 5.17	14.59 $\pm$ 0.41
VzqfbhrpDEA	27.41 $\pm$ 2.28	15.64 $\pm$ 0.72	396.57 $\pm$ 6.72	9.19 $\pm$ 0.40
X7HyMhZNoso	62.86 $\pm$ 1.17	29.77 $\pm$ 1.18	278.76 $\pm$ 4.89	4.16 $\pm$ 0.42
Z6MFQCViBuw	47.33 $\pm$ 3.40	15.48 $\pm$ 1.83	368.63 $\pm$ 8.25	5.93 $\pm$ 0.66
gTV8FGcVJC9	50.00 $\pm$ 1.63	27.88 $\pm$ 2.24	316.60 $\pm$ 11.00	7.03 $\pm$ 0.44
gYvKGZ5eRqb	18.33 $\pm$ 2.36	3.68 $\pm$ 0.50	468.87 $\pm$ 6.26	9.14 $\pm$ 1.13
oLBMNvg9in8	47.67 $\pm$ 1.70	27.95 $\pm$ 2.42	322.73 $\pm$ 10.51	3.65 $\pm$ 0.08
pLe4wQe7qrG	51.11 $\pm$ 1.57	26.30 $\pm$ 4.24	317.16 $\pm$ 15.91	3.56 $\pm$ 0.22
pa4otMbVnkk	31.11 $\pm$ 9.56	13.82 $\pm$ 3.98	398.71 $\pm$ 26.33	9.85 $\pm$ 1.45
rqfALeAoiTq	38.61 $\pm$ 3.22	18.14 $\pm$ 1.66	369.56 $\pm$ 11.93	4.89 $\pm$ 0.11
x8F5xyUWy9e	50.00 $\pm$ 3.40	21.01 $\pm$ 1.50	332.68 $\pm$ 12.40	4.41 $\pm$ 0.13
yqstnuAEVhm	41.11 $\pm$ 2.39	18.79 $\pm$ 1.28	363.67 $\pm$ 11.33	4.81 $\pm$ 0.08
zsNo4HB9uLZ	28.75 $\pm$ 2.70	16.22 $\pm$ 0.45	399.03 $\pm$ 8.76	6.50 $\pm$ 0.24
Average	37.80	18.25	372.41	6.67

### 10. Social Impact and Future Work

We see our work as a starting point to propose a general and scalable method to offline learn a navigation policy from limited sources for any mobile agents. In the future, We believe NOLO will benefit a lot from the rapid development in optical flow and computer vision foundation models, and there will be extensive applications of NOLO, such as deployment to sweeping robots or rescue robots. Further improvement can be conducted to examine and enhance the reliability of the decoded actions from optical flow. It is also a great idea to incorporate first-person and third-person videos to showcase more advanced intelligence of spatial understanding and egocentric decision-making in more complex 3D embodied environments.